Article

SOURCE DATA | TRANSPARENT PROCESS | OPEN ACCESS

EMBO reports

# Bacteria-instructed B cells cross-prime naïve CD8$^+$ T cells triggering effective cytotoxic responses

Raquel García-Ferreras[1], Jesús Osuna-Pérez[1], Guillermo Ramírez-Santiago[1], Almudena Méndez-Pérez[1], Andrés M Acosta-Moreno[1], Lara Del Campo[1,2], María J Gómez-Sánchez[1,3], Marta Iborra[4], Beatriz Herrero-Fernández[5,6], José M González-Granado[5,7,8], Francisco Sánchez-Madrid[5,9,10], Yolanda R Carrasco[11], Patricia Boya[12], Nuria Martínez-Martín[4] & Esteban Veiga[1,*]

## Abstract

**In addition to triggering humoral responses, conventional B cells have been described *in vitro* to cross-present exogenous antigens activating naïve CD8$^+$ T cells. Nevertheless, the way B cells capture these exogenous antigens and the physiological roles of B cell-mediated cross-presentation remain poorly explored. Here, we show that B cells capture bacteria by trans-phagocytosis from previously infected dendritic cells (DC) when they are in close contact. Bacterial encounter "instructs" the B cells to acquire antigen cross-presentation abilities, in a process that involves autophagy. Bacteria-instructed B cells, henceforth referred to as BacB cells, rapidly degrade phagocytosed bacteria, process bacterial antigens and cross-prime naïve CD8$^+$ T cells which differentiate into specific cytotoxic cells that efficiently control bacterial infections. Moreover, a proof-of-concept experiment shows that BacB cells that have captured bacteria expressing tumor antigens could be useful as novel cellular immunotherapies against cancer.**

**Keywords** B cell-mediated antigen cross-presentation; cancer immunotherapy; cellular therapy; *Listeria monocytogenes*; transphagocytosis
**Subject Categories** Autophagy & Cell Death; Immunology; Microbiology, Virology & Host Pathogen Interaction
**DOI** 10.15252/embr.202256131 | Received 14 September 2022 | Revised 14 April 2023 | Accepted 25 April 2023 | Published online 15 May 2023
**EMBO Reports (2023) 24: e56131**

## Introduction

B cells play crucial roles during immune responses to pathogen or tumor insults, however, their functions outside the humoral responses are poorly understood. The major role of B cells is to orchestrate humoral immunity to generate high-affinity antibodies against antigens (Nutt *et al*, 2015). The first step in this response begins with the recognition of foreign antigens e.g. soluble or particulate antigens and large immune complexes, by the B cell receptor (BCR) (Yang & Reth, 2010; Mattila *et al*, 2013; Liu *et al*, 2016). B cells mainly recognize the unprocessed antigens on the surface of antigen presenting cells (APCs) such as subscapular sinus macrophages (Carrasco & Batista, 2007; You *et al*, 2011; Prokopec *et al*, 2016), dendritic cells (DCs) (Qi *et al*, 2006; Gonzalez *et al*, 2010) and follicular dendritic cells (FDCs) (Suzuki *et al*, 2009). Antigen exposition produces a BCR microcluster formation that finishes with the antigen internalization by B cells (Fleire *et al*, 2006; Yuseff *et al*, 2011; Natkanski *et al*, 2013). In addition, small soluble antigens can also rapidly access the B cell compartment of the secondary lymph organs through conduits (Roozendaal *et al*, 2009). The BCR-mediated extraction of antigens allows the B cells to present them to the CD4$^+$ T cells in the T-B border of the lymph nodes (Garside *et al*, 1998; Allen *et al*, 2007; Crotty, 2019). Consequently, the CD4$^+$ T cell contacts provide the necessary signals for the B cells to become fully activated and to produce a full humoral immune response (Akkaya *et al*, 2020).

Some studies suggest that B cells can be also involved in cross-presentation, activating naïve CD8$^+$ T cells (de Wit *et al*, 2010;

1 Department of Molecular & Cellular Biology, Centro Nacional de Biotecnología, Consejo Superior de Investigaciones Científicas (CNB-CSIC), Madrid, Spain
2 Departamento de Biología Celular, Facultad de Odontología, Universidad Complutense de Madrid, Madrid, Spain
3 Department of Immunology, School of Medicine, Complutense University of Madrid, 12 de Octubre Health Research Institute (imas12), Madrid, Spain
4 Centro de Biología Molecular Severo Ochoa (CSIC-UAM), Madrid, Spain
5 LamImSys Lab, Instituto de Investigación Hospital 12 de Octubre (imas12), Madrid, Spain
6 Departamento de Fisiología, Facultad de Medicina, Universidad Autónoma de Madrid (UAM), Madrid, Spain
7 CIBER de Enfermedades Cardiovasculares, Instituto de Salud Carlos III, Madrid, Spain
8 Department of Immunology, Ophthalmology and ENT, School of Medicine, Universidad Complutense de Madrid, Madrid, Spain
9 Centro Nacional de Investigaciones Cardiovasculares (CNIC), Madrid, Spain
10 Hospital Universitario de la Princesa, Instituto Investigación Sanitaria Princesa (IIS-IP), Universidad Autónoma de Madrid, Madrid, Spain
11 Department of Immunology & Oncology, Centro Nacional de Biotecnología, Consejo Superior de Investigaciones Científicas (CNB-CSIC), Madrid, Spain
12 Department of Neuroscience, University of Fribourg, Fribourg, Switzerland
*Corresponding author. Tel: +34 915854548; E-mail: eveiga@cnb.csic.es

Alloatti *et al*, 2015; Ren *et al*, 2021) despite the general belief indicating that cross-presentation is mainly carried out by certain subtypes of DC (Cerovic *et al*, 2015; Wculek *et al*, 2020; Canton *et al*, 2021). Increasing evidence has shown that DC-mediated cross-presentation is crucial to triggering the $CD8^+$ T cells responses necessary to clean viral infections (Wu *et al*, 2019; Barbet *et al*, 2021) and to fight against tumors (Sánchez-Paulete *et al*, 2017; Wculek *et al*, 2020).

It is not clear, however, how B cells capture and process the cross-presented antigens, neither the physiological role of such B-cell mediated antigen cross-presentation. In this regard, recent studies have shown that B cells infiltration in tumors is correlated with good prognosis and it has been suggested that this could be related to the antigen presentation ability of B cells (Garnelo *et al*, 2017; Edin *et al*, 2019; Lu *et al*, 2020; Hu *et al*, 2021).

It is well known that professional phagocytes like DCs usually internalize pathogens by phagocytosis (Gordon, 2016). Similarly, B cells from early vertebrates are able to phagocytose pathogens (Li *et al*, 2006). Mammals maintain this innate capacity in certain B cell subsets (B1 B cells) (Gao *et al*, 2012). However, it is widely accepted that conventional B cells (B2 cells), the most common type of B cells in the spleen, do not have phagocytic abilities (Ochando *et al*, 2006). Indeed, they are commonly used as negative controls in phagocytosis experiments (Vidard *et al*, 1996; Ochando *et al*, 2006). Contrary to this theory, some authors have shown that conventional B cells phagocytose antigens through their BCR and initiate a humoral response against those antigens (Martínez-Riaño *et al*, 2018). In addition, other investigations have reported the capture of *Salmonella in vitro* by conventional B cells (Rosales-Reyes *et al*, 2012; Souwer *et al*, 2012). Consequently, there is not a clear consensus about whether mammalian conventional B cells are phagocytic cells neither their ability to process and present antigens from captured pathogens.

We previously described that the non-phagocytic $CD4^+$ T cells, are able to capture bacteria by a process termed trans-phagocytosis from infected DCs (Cruz-Adalia *et al*, 2014, 2017), similarly to what is observed for several viruses (Holl *et al*, 2010; Gaspar *et al*, 2011). Likewise, it has been shown that infected DCs, which are unable to completely destroy the uptaken bacteria (Campisi *et al*, 2011) migrate towards the lymph nodes, where they establish stable contacts with B cells (Waite *et al*, 2011), which could favor bacterial uptake by B cells. However, the ability of the B cells to capture bacteria from infected DCs by trans-phagocytosis, which could be a source to provide antigens for cross-presentation, has not yet been explored.

In this study we show that conventional B cells are able to capture bacteria by trans-phagocytosis while forming immunological contacts with infected DCs. We also show that these captured bacteria are a source of cross-presented antigens. Exposure to bacteria instructs B cells (BacB cells) that acquired the ability of cross-present bacterial antigens, being able to destroy internalized bacteria, process bacterial antigens and cross-present these antigens activating naïve $CD8^+$ T cells, which in turn, trigger a potent cytotoxic response. The antigen cross-presentation ability of BacB cells, which requires active autophagy, drives the activation of $CD8^+$ T cells involved in the resolution of pathogen infection and the elimination of implanted tumors. These results pave the way for future research regarding the use of BacB cells as a potential novel generation of cellular immunotherapy against cancer.

## Results and Discussion

### B cells capture bacteria by trans-phagocytosis from infected dendritic cells

A controversy exists regarding the ability of conventional B cells to phagocytose bacteria (Menon *et al*, 2003; Krocova *et al*, 2020). Although some studies suggest that they induce potent $CD8^+$ T cells responses during infection (Khanna *et al*, 2007), the way that B cells capture antigens for $CD8^+$ T cells activation has not yet been described. As a response to this lack of consensus, we have studied the capacity of B cells to capture *Listeria monocytogenes*, a bacterium model that induces $CD8^+$ T cell cellular immunity (Chávez-Arroyo & Portnoy, 2020; Levine *et al*, 2021).

Conventional B cells ($CD19^+$ $CD5^-$; Fig EV1A) were purified from mouse spleen to test their ability to capture bacteria. Conventional B cells *in vitro* were refractory to direct bacteria capture, even though *L. monocytogenes* is a pathogen able to infect non-phagocytic cells. On the contrary, professional phagocytes such as BM-DCs were able to capture *L. monocytogenes* (Fig 1A). Next, we enabled immunological contact between infected BM-DCs (iDCs) and conventional B cells. To mimic immune synapses, we used the well-known MD4-HEL model. B cells were obtained from MD4 mice, expressing a BCR that recognizes Hen Egg Lysozyme (HEL). HEL-decorated BM-DCs were infected with *L. monocytogenes*, and co-incubated with MD4 B cells. The subcellular localization of *Listeria* during iDCs/B cell contacts was imaged by confocal microscopy. During early immunological synapse formation, i.e occurred within 30 min, the bacteria inside iDCs polarized towards cell-to-cell contacts (Fig 1B). Extended (2 h) iDC/B cell immunological synapses showed that B cells were able to capture bacteria (Fig 1C, Movie EV1).

The process of bacterial capture by B cells from infected DC (transphagocytosis) was further quantified by classical gentamicin survival assays as described (Cruz-Adalia *et al*, 2014). B cells, were re-isolated 90 min after iDC/B cells conjugate formation. Gentamicin was added to the medium 30 min after cell–cell contacts and left for an additional 60 min to kill extracellular bacteria; under the conditions used, gentamicin does not permeate inside B cells. Then, B cells were lysed and the intracellular content was plated in BHI (Brain Heart Infusion) agar plates. After 48 h incubation at 37°C the bacterial colonies were counted, whereby each colony represented one live intracellular bacterium. Direct bacterial capture by B cells was used as negative control. The possible requirement of cell-to-cell contact was investigated using polycarbonate filter-containing chambers of 3 μm pore size (Transwell) which impedes cellular contact between the iDCs and B cells, but allows the passage of bacteria. The possible role of BCR activation by their cognate antigen was tested by decorating (or not) the DC cells with HEL which is recognized by BCR of MD4 B cells.

B cells need physical contact with iDCs in order to capture bacteria (Fig 1D); in the presence of a physical barrier preventing cell-to-cell contact, but allowing bacterial dissemination, no bacterial capture was detected. BCR activation, by the presence of HEL at DC surface, is not necessary for bacterial capture (Fig EV1B and C, Movies EV2 and EV3), but increased about three-fold the bacterial uptake compared with the absence of antigen at the time measured

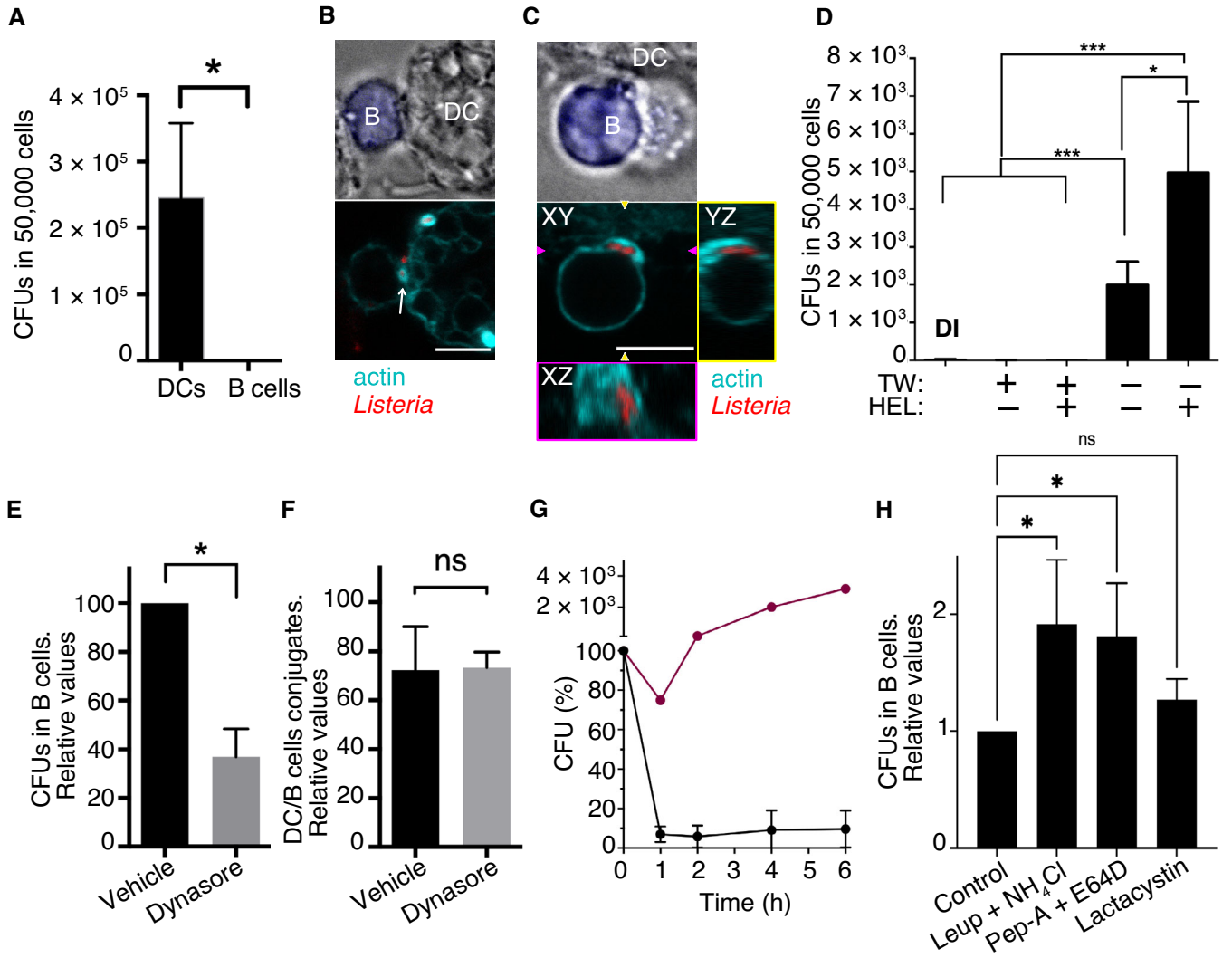


**Figure 1. B cells capture bacteria by trans-phagocytosis.**

A Gentamicin survival assay showing bacteria captured by DC or B cells.

B, C Confocal images of DCs decorated with HEL (not colored) infected with *L. moncytogenes* (in red), coincubated during 30 min (B) or 120 min (C) with noninfected B cells (in blue) isolated from MD4 mice. Actin is shown in cyan. In (C), the orthogonal views show intracellular bacteria in B cell. Scale bars represent 5 μm. White arrow in (B) point to a bacterium at the B cell-DC contact area surrounded by actin. Arrowheads in (C) indicate the XZ and YZ axes.

D *L. monocytogenes*-infected DCs were decorated (or not) with HEL, followed by coincubation B cells in conditions that allow DC-B cell contacts or in the presence of a phisical barrier (transwell) preventing cellular interactions. After conjugate formation (90 min), B cells were reisolated, and intracellular bacteria in B cells were measured by classical gentamicin survival assays.

E Gentamicin survival assay showing bacteria captured by B cells treated or not whith 80 μM Dynasore.

F Quantification of DC/B cells conjugate formation afer dynasore treatmeted of B cells. Data were normalized compared to DC/B cells conjugates without treatment (vehicle).

G Bacteria-infected and HEL-loaded DCs were co-incubated with B cells from MD4 mouse. After conjugate formation, BacB cells were re-isolated, and intracellular bacteria were detected by gentamicin survival assays at different times. Data were normalized compared to time 0. As control of the bacterial fitness, in parallel, HeLa cells were directly infected.

H WT B cells were allowed to form conjugates with *Listeria*-infected DC, after 30 min samples were treated with the indicated inhibitors; Leupeptin + $NH_4Cl$, pepstatin-A + E64D, lactacystin, or PBS for controls. One hour later gentamicin was added to kill extracellular bacteria and 2 h later B cells were reisolated by negative selection, lysed and plated in agar-containing plates. CFUs were counted; each colony represents one live intracellular bacterium inside B cells.

Data information: Column bars in the figure represent the mean of at least three independent experiments. Error bars indicate the SD. Significant differences, analyzed by *t*-test (two samples) or one way ANOVA (more than two samples), are represented by asterisk; *$P < 0.05$, ***$P < 0.0005$, non-significant differences are marked as (ns). Source data are available online for this figure.

i.e. 90 min DC/B cells contacts (Fig 1D). B cells treated with a pharmacological inhibitor of dynamin, dynasore, before iDC/B coculture showed a decrease in bacteria capture (Fig 1E), indicating that transphagocytic process requires the cellular endocytic machinery. The treatment of B cells with dynasore does not impede DC/B cell immune contacts (Fig 1F).

Bacterial viability following capture by B cells was analyzed using gentamicin survival assays at different time intervals. The B cells rapidly killed the internalized bacteria (Fig 1G). Indeed, B cells destroyed more than 95% of the internalized *L. monocytogenes* in the first hour. As a control for the measure of bacterial fitness, *L. monocytogenes* infection of HeLa cells was monitored, and showed intracellular bacterial growth (Fig 1G). These combined results show that B cells capture bacteria by trans-phagocytosis during contact with infected DCs and efficiently destroy the uptaken bacteria. The presence of leupeptin (inhibitor of cysteine, serine and threonine peptidases in lysosomes) and ammonium chloride (which inhibits the acidic degradation in the lysosomes) partially inhibit bacterial degradation by B cells (Fig 1H). Likewise, the combination of Pepstatin A and E64D, (inhibitors of Cathepsins D and B respectively) also partially inhibits bacteria degradation, suggesting that lysosome degradation plays an important role in intracellular bacterial clearance in B cells. On the contrary, the presence of proteasome inhibitor (lactacystin) does not impede bacterial degradation (Fig 1H). Our results matched with previous observations about the requirement of endosomal acidification, proteasomal processing and classical MHC class-I/peptide transport for cross-presentation by B cells (Robson *et al*, 2008).

In addition, supporting the active role played by B cells in bacterial capture, and ruling out the necessity of bacterial virulence factors in the transphagocytosis process, we observed that B cells are able to capture pathogen (*L. monocytogenes*) and non-pathogen (*Escherichia coli*) bacteria (Fig EV1D).

### B cells capturing bacteria establish mature immune synapses with naïve CD8$^+$ T cells

We investigated whether B cells can process and cross-present antigens from captured bacteria. The expression levels of co-stimulatory molecules CD80 and CD86, which are necessary for effective antigen presentation, as well as MHC-I (H-2K$^b$ haplotype) were analyzed in B cells after 24 h of iDC/B cells contacts. Co-stimulatory molecules and H-2K$^b$ increased on the surface of B cells after *L. monocytogenes* uptake (Fig 2A–F).

In order to quantify bacteria capture and antigen processing/presentation of bacteria antigens by B cells, we generated a *L. monocytogenes* strain that constitutively expressed ovalbumin (*Listeria*-OVA). After 24 h of iDC/B cells contacts, the B cell population presented the OVA peptide SIINFEKL (OVA-pI) on MHC class I (Fig 2G and H). These data indicated that by increasing the cell-to-cell contact time to 24 h, a large majority of B cells had captured bacteria, processed and presented bacterial antigens, i.e. OVA, indicating that bacteria capture and antigen cross-presentation is a massive event.

The hallmark of naïve CD8$^+$ T cell activation by the antigen presenter APC is the formation of a functional structure, formed at the cell-to-cell contact, which is termed immunological synapsis (IS; Dustin & Depoil, 2011). The IS refers to an area of intimate contact between T cells and APCs presenting antigens recognized specifically by the T cell receptor (TCR), where signals are coordinated, and integrated to support T cell activation. The mature IS architecture is commonly divided into areas known as Supra Molecular Activation Clusters (SMAC). The T Cell Receptor (TCR) and other signaling molecules accumulate in the central area of the SMAC (cSMAC). This cSMAC is surrounded by the peripheral SMAC (pSMAC) accumulating integrin LFA-1 and massive quantities of F-actin that is the signature of IS formation and the first step in CD8$^+$ T cell activation (Huppa & Davis, 2003; Calabia-Linares *et al*, 2011). Naïve CD8$^+$ T cells isolated from OTI transgenic mice, which express a TCR that recognizes ovalbumin peptide (OVA-pI 256–264; SIINFEKL) in the context of the H-2K$^b$ MHC-I haplotype, were co incubated with B cells capturing either *Listeria*-OVA or its isogenic wild-type strain (*Listeria*-WT). Immunofluorescence microscopy analysis confirmed that naïve OTI CD8$^+$ T cells established mature IS when were in contact with B cells that have captured *Listeria*-OVA but not when B cells captured *Listeria*-WT (Fig 2I). When OTI CD8$^+$ T cells contacted B cells that captured *Listeria*-OVA the accumulation of CD3 and F-actin were clearly visible at the IS (Fig 2I right panels) as well as the typical actin ring formed in the pSMAC (Movies EV4–EV6). By contrast, when B cells have captured *Listeria*-WT they rarely made contacts with OTI CD8$^+$ T cells, and no sign of IS formation was detected (Fig 2I left panels). Quantification of actin accumulation at the IS using the plugin of imageJ "synapse measures" on confocal images (Calabia-Linares *et al*, 2011), confirmed that B cells capturing *Listeria*-OVA, but not B cells capturing *Listeria*-WT induced massive actin polymerization on contact with naïve OTI CD8$^+$ T cells (Fig 2J).

### BacB cells cross-present bacterial antigens, activating naïve CD8$^+$ T cells

Antigen cross-presentation is important for the activation of naïve CD8$^+$ T cells and the generation of a cytotoxic response. It is widely believed that only some DCs subsets have the ability to cross-present antigens. Contrary to this theory, several reports have shown that B cells can cross-present external antigens. Coupling the TLR9 ligand CpG to OVA enhanced non-cognate B cell endocytosis ability and promoted B cell activation. CpG-OVA complex-loaded B cells cross-primed CD8 T cells *in vivo* (Heit *et al*, 2004). Using plasmid-encode antigen as a DNA vaccination tool, Hon *et al* (2005) found that B cells mediate cross-priming of antigen-specific CD8$^+$ T cells. Furthermore, BCR-recognition of specific antigen drove an efficient antigen uptake and cross-presentation in MHC class-I, stimulating CD8$^+$ T cells responses *in vitro* comparable to those ones elicited by bone marrow-derived DCs (Robson *et al*, 2008). The authors used immune-stimulating complexes where OVA and HEL proteins were incorporated to stimulate HEL-specific B cells and, thus, the uptake of immune complexes triggered by cognate BCR/antigen interactions. Immunization studies indicated that HEL-specific B cells have a major role in maintaining the clonal expansion of OVA-specific CD8$^+$ T cells (Robson *et al*, 2008). This study set up the groundwork of targeting B cells for promoting CD8$^+$ T cell responses as a therapeutic tool. In agreement with these studies, mouse B cells have been shown to prime antigen specific cytotoxic response following DNA stimulation better than DCs *in vivo* (Colluru & McNeel, 2016). Besides, Mariño *et al* (2012) found in an autoimmune mouse model of diabetes that B cells cross-present autoantigens to self-reactive CD8$^+$ T cells by MHC class-I and BCR-dependent mechanisms. Moreover, a previous study found that cross-presentation of *Salmonella* antigens by B cells result in the activation of a CD8$^+$ cytotoxic T cell response *in vitro*, requiring the help of CD4$^+$

T cells. The mechanism of cross-presentation of Salmonella antigens by B cells is however unknown (de Wit *et al*, 2010).

To assess the antigen-crosspresenting capacity of B cells capturing bacteria, DCs were infected with either *Listeria*-OVA or its isogenic wild-type strain, *Listeria*-WT. iDCs were cultivated together with non-infected B cells overnight. Then, B cells were repurified by cell sorting (Fig EV2A) and tested for antigen presentation to naive OTI CD8$^+$ T cells. Note that bacterial instruction requires at least 24 h and most of the DC died after 24 in the presence of *Listeria* (Fig EV2B), surprisingly B cells are more resistant. Flow cytometry analysis (Fig EV2C) of OTI CD8$^+$ T cell proliferation showed a robust proliferation only when B cells have captured *Listeria*-OVA (Fig 3A and B). OTI CD8$^+$ T cells incubated with B cell that have captured *Listeria*-WT did not proliferate (Fig 3A and B).

Together, these results show that bacterial exposure "instructs" B cells (From now on termed bacteria instructed B cells; BacB) that acquire antigen cross-presentation abilities, and confirmed the specificity of BacB-mediated antigen cross-presentation.

The activation of naïve OTI CD8$^+$ T cells was confirmed by the upregulation of the activation marker CD25 (Fig 3C and D). This

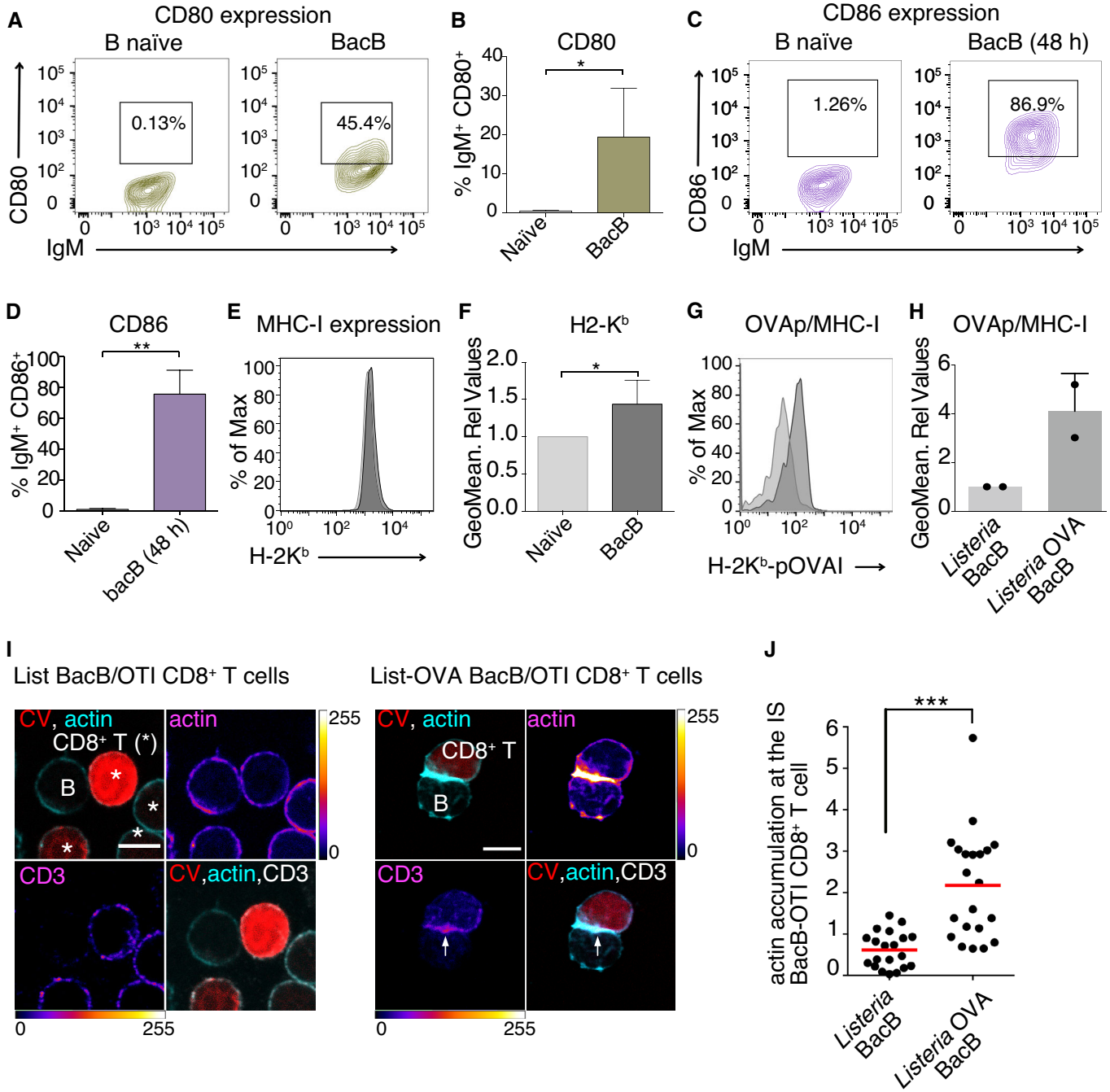


**Figure 2.**

**Figure 2. *L. monocytogenes* capture instructs B cells to become antigen cross-presenting cells.**

A–D CD80 (A, B) and CD86 (C, D) expression in B cells measured by flow cytometry on day 0 (non-instructed; naïve) and day 2 after *L. monocytogenes* capture (BacB). (A and C) show representative experiments, (B and D) show the mean of at least three independent experiments.

E, F H-2K$^b$ expression in B cells measured by flow cytometry on day 0 (naïve, pale gray) and day 1 after *L. monocytogenes* capture (BacB; dark gray). (E) Shows a representative experiment, (F) shows the mean of four independent experiments.

G, H Expression of OVAp-I in the context of H-2K$^b$ was detected by flow cytometry with anti-OVAp-I/H-2K$^b$ antibody, comparing BacB capturing *Listeria*-WT (pale gray) and *Listeria*-OVA (dark gray). (G) Shows a representative experiment, (H) shows the mean of two independent experiments.

I Confocal images of *Listeria*-WT (left panels) or *Listeria*-OVA (right panels) BacB cells incubated with naïve OTI CD8$^+$ T cells previously stained with CellTraceViolet (CV, red). Actin and CD3 fluorescence are shown on a "fire" scale and in cyan and white respectively in the merged images. Scale bars = 10 μm. *Indicate CD8$^+$ T cells. Arrow points to the IS.

J Quantification of actin accumulation at the IS on CD8$^+$ T cells conjugated with *Listeria*-WT or *Listeria*-OVA BacB cells, analyzed using *Synapse measures* software from confocal images. Each dot corresponds to one IS. Three independent experiments were performed.

Data information: Column bars in the figure represent the mean. Error bars indicate the SD. Significant differences, analyzed by *t*-test are represented by asterisk; *$P < 0.05$, ***$P < 0.0005$, non-significant differences are marked as (ns).
Source data are available online for this figure.

increase in CD25$^{high}$ OTI CD8$^+$ T cell population was only observed when the APCs were BacB cells that have captured *Listeria*-OVA (*Listeria*-OVA BacB), but not when APCs were *Listeria*-WT BacB cells. OTI CD8$^+$ T cells that have been activated by *Listeria*-OVA BacB cells, showed proliferations levels comparable, and even larger, than those generated by the positive controls of T cell proliferation, i.e. BM-DC decorated with soluble OVA-pI (as bacteria exposure damage BM-DC, we used LPS-activated, OVApI-decorated DC to maximize its antigen presenting ability) and polyclonal T-cell activation using anti CD3/CD28 antibodies (Fig 3E and F). Therefore, BacB-mediated antigen presentation induce a potent activation of naïve CD8$^+$ T cells. Likewise, BacB-mediated CD8$^+$ T cell activation was also observed using B cells isolated from WT mice in absence specific BCR activation (Fig EV3A and below throughout the manuscript) confirming that transphagocytosis and bacteria-induced instruction does not require BCR engagement. We found no major differences in antigen cross-presentation abilities of BacB cells from WT or MD4 mice (HEL-activated). We decided, therefore, to use WT B cells which is a more physiological setting that MD4 B cells/HEL decorated DC.

We further investigated whether BacB cells process endogenously bacterial antigens to induce CD8$^+$ T cell proliferation, or whether BacB cells capture MHC molecules from DC during the trans-phagocytosis process by trogocytosis (Schriek *et al*, 2022). OTI CD8$^+$ T cells were incubated with *Listeria*-OVA BacB cells (expressing H-2K$^b$ MHC-I haplotype). In these experiments, the B cells captured bacteria from BM-DCs expressing either H-2K$^b$ or H-2K$^k$ MCH-I haplotypes. Note that OTI CD8$^+$ T cells recognize OVAp in the context of H-2K$^b$ haplotype and therefore APCs expressing H-2K$^k$ are unable to activate OTI CD8$^+$ T cells. OTI CD8$^+$ T cell proliferation was similar in both conditions (Fig 3G and H), supporting the hypothesis that BacB cells are able to process antigens endogenously. In agreement, OTI CD8$^+$ T cell proliferation was reduced when the antigen presentation was mediated by Tap1$^{-/-}$ BacB cells, compared to that observed when wild-type BacB cells were used (Fig EV3B) indicating that BacB cells, similarly to what was observed in DC (Blander, 2018) and CD4$^+$ T cells (Cruz-Adalia *et al*, 2017), use the Tap-dependent, canonical way (Barbet *et al*, 2021), as the major cross-presentation pathway.

Finally, we tested whether BacB cell-mediated antigen presentation induced the differentiation of naïve CD8$^+$ T cells into cytotoxic effector cells. OTI CD8$^+$ T cells cross-primed with *Listeria*-OVA BacB cells eliminated OVApI-expressing EL-4 lymphoma target cells (Lang *et al*, 2005) more efficiently than OT-I CD8$^+$ T cells activated by splenocytes (Fig 3I), highlighting the capacity of BacB cells to generate potent cytotoxic effector CD8$^+$ T cells. In agreement with these data, BacB-mediated activation of naïve CD8$^+$ T triggers the expression granzyme B, perforin and interferon gamma IFN-γ (Fig 3J–L), which are involved in the cytotoxic activity of CD8$^+$ T cells (Tau *et al*, 2001), at similar and even higher levels than observed in CD8$^+$ T cells activated by using anti CD3 and anti CD28 antibodies or by OVA-decorated splenocytes (positive controls).

Together, these *in vitro* results show that bacteria capture by transphagocytosis is a source of antigens for BacB cells, that cross-prime naïve CD8$^+$ T cells, inducing their differentiation into effective cytotoxic T cells (CTLs).

## Autophagy is necessary for bacteria-mediated instruction of bacB cells

Autophagy has emerged as an important function in processing antigens presented via the major histocompatibility complex class I (MHC I) (English *et al*, 2009; Mintern *et al*, 2015; Parekh *et al*, 2017) and MCH II (Paludan *et al*, 2005; Schmid *et al*, 2007; Münz, 2016), as well as regarding the innate immune response to pathogens (Germic *et al*, 2019; Tao & Drexler, 2020). Pathogens and pathogen-containing vacuoles can be marked by "eat-me" signals that trigger the xenophagy, a type of non-canonical autophagy that targets intracellular pathogens for lysosomal degradation (Gutierrez *et al*, 2004; Pilli *et al*, 2012; Wang *et al*, 2020). Studies of *Listeria* infection in non-phagocytic cells as well as professional phagocytes have shown that intracellular *L. monocytogenes* triggers the cellular autophagy (Anand *et al*, 2011; Mitchell *et al*, 2018).

We analyzed whether bacteria described to trigger autophagy could be involved in the B cell instructing process using B cells isolated from WT mice. BacB cells capturing different bacteria were assessed for their APC capacity by measuring CD80 and H-2K$^b$ expression. B cells capturing *E. coli* (bacteria that do not trigger autophagy) expressed lower levels of H-2K$^b$ or CD80 than *Listeria* BacB cells (Fig 4A–D). Accordingly, *E. coli*-OVA BacB cells were unable to form mature IS with OT-I CD8$^+$ T cells (Fig EV3C and D) neither induce the proliferation of OT-I CD8$^+$ T cells (Fig 4E and F).

There are obvious differences in PAMPs (Pathogen Associated Molecular Patterns) expression between *E. coli* and *L. monocytogenes* which are Gram− and Gram+ respectively. These bacteria show also

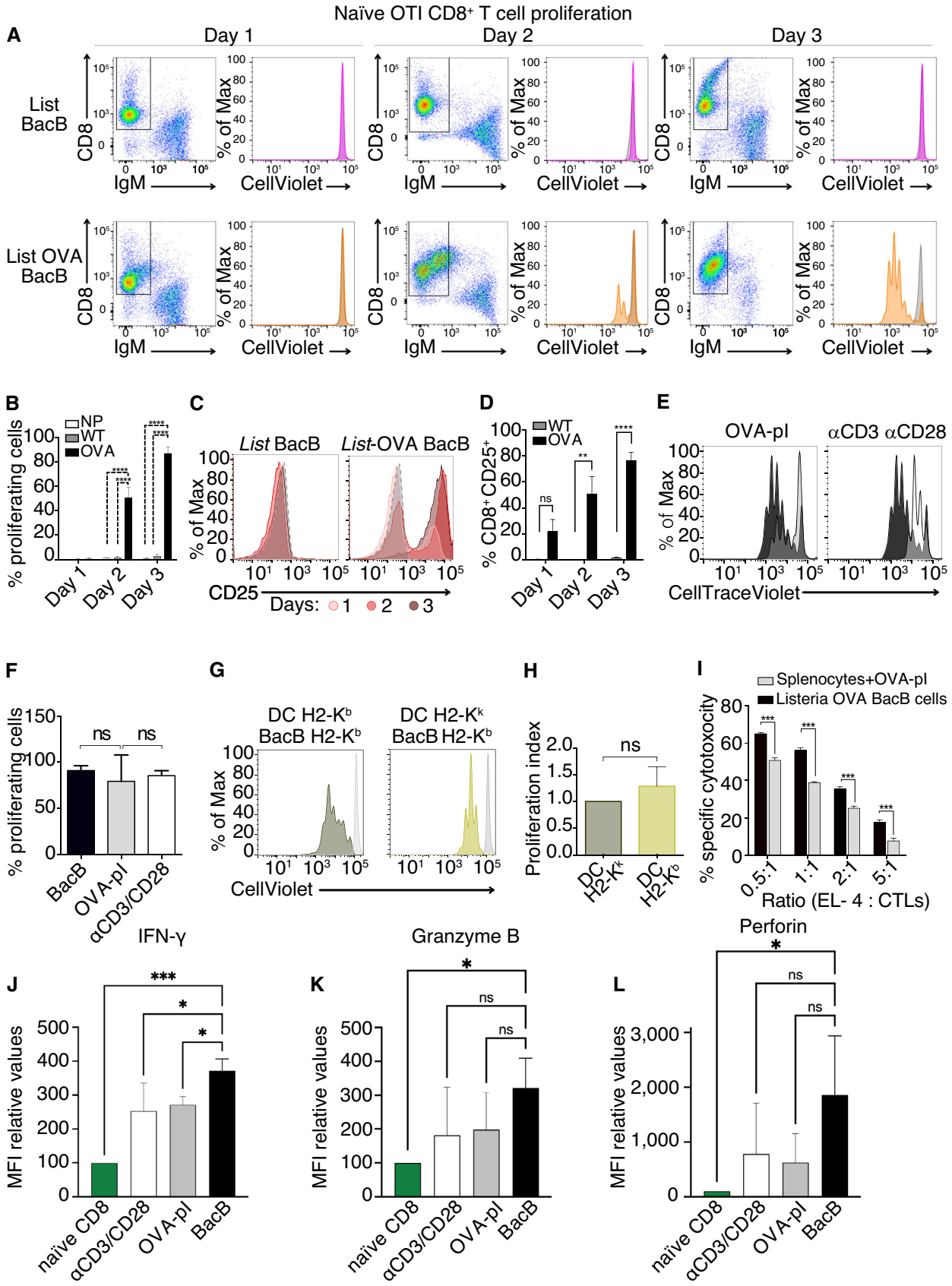


**Figure 3.**

**Figure 3. BacB cells process antigens from captured bacteria and cross-prime na45ve CD8$^+$ T cells.**

A Representative experiments showing naïve OTI CD8$^+$ T cell proliferation measured by flow citometry 1, 2 or 3 days after *Listeria*-WT (top panels) or *Listeria*-OVA (bottom) BacB cell contacts. The histograms show CellTrace Violet stain dilution (proliferation) corresponding to CD8$^+$ T cell population (CD8$^+$, IgM$^-$). Non-activated naïve CD8$^+$ T cells (thin gray line) are shown as a negative proliferation control.

B Mean of at least three experiments showing the % of naïve OTI CD8$^+$ T cell proliferated after activation (days 1–3) with BacB capturing *Listeria*-WT (WT) or *Listeria* OVA (OVA). Non-activated, non-proliferative CD8$^+$ T cells (NP) are shown as control.

C, D CD25 expression in OTI CD8$^+$ T cells on day 1 (light red), day 2 (red) and day 3 (dark red) after activation with *Listeria*-WT (left panel) or *Listeria*-OVA (right panel) BacB cells. FMO control is shown in gray and dash line. (C) Representative experient. (D) Mean of at least three independent experiments.

E Representative experiment showing OT-I CD8$^+$ T cells proliferation measured at day 3 after activation with OVAp-I-loaded BM-DCs (left panel, light gray) or by polyclonal activation using CD3/CD28 antibodies (right panel, light gray) compared in parallel with *Listeria*-OVA BacB-mediated activaton (dark gray in both panels).

F Mean of at least three experiments showing the % of naïve OTI CD8$^+$ T cell proliferated after activation as in (D).

G, H Proliferation of OTI CD8$^+$ T cells activated with *Listeria*-OVA BacB cells (H-2K$^b$) that captured bacteria from infected H-2K$^b$ or H-2K$^k$ iBM-DCs. Non-activated naïve CD8$^+$ T cells are shown (thin gray line). B cells were isoated from WT mice. (G) Shows a representative experiment, (H) shows the mean of the proliferation index from at least three independent experiments (relative to H-2K$^k$ iBM-DCs donor cells).

I Relative specific cytotoxicity of effector CD8$^+$ T cells (CTL) generated after activation with *Listeria*-OVA BacB cells (black) or OVAp-I-loaded splenocytes (gray). Various OVA loaded EL-4 (target cell):CTL ratios were measured. It is shown the mean of four independent experiments (biological replicates).

J–L Intracellular expression, measured by flow cytometry, of the indicated proteins in non-activated, naïve, CD8$^+$ T cells or in CD8$^+$ T cells activated with either antiCD3 + antiCD28 antibodies (αCD3/CD28), OVA-decorated splenocytes (OVA-pI), or *Listeria*-OVA BacB cells (BacB). The mean fluorescence intensity and the sd corresponding to three independent experiments is shown.

Data information: Column bars in the figure represent the mean of at least three independent experiments. Error bars indicate the SD. Statistical significant differences analyzed by one-way ANOVA is represented by asterisk. *$P < 0.05$, ***$P < 0.0005$, non-significant differences are marked as (ns).
Source data are available online for this figure.

very different behavior, being pathogen (*L. monocytogenes*) and non-pathogen (*E. coli*).

Listerolysin O (LLO; encoding by the hly gene) is an essential virulent factor of *L. monocytogenes* which triggers cellular autophagy (Meyer-Morse *et al*, 2010; Mitchell *et al*, 2018). We, therefore, also analyzed the antigen cross-presenting abilities of BacB cells that have captured LLO-deficient *L. monocytogenes* expressing OVA (*Listeria* Δhly OVA), and compared to what is observed using its isogenic WT strain. *Listeria* Δhly OVA BacB cells were unable to establish functional IS with naïve OTI CD8$^+$ T (Fig EV3E and F) nor regulate CD80 or H-2K$^b$ expression (Fig 4G–J) or induce proliferation of naïve OT-I CD8$^+$ T cells (Fig 4K and L). Complementation assays allowing the expression of LLO in *Listeria* Δhly (*Listeria*Δhly::hly OVA; Fig EV3G) show the recovery of the phenotype of *Listeria*-OVA BacB cells. *Listeria*Δhly::hly OVA BacB cells were able to efficiently activate OT-I CD8$^+$ T cells (Fig 4M and N).

In order to analyze the autophagic flux in BacB cells and to determine whether bacteria internalization triggers canonical or non-canonical autophagy we followed the protocol as described in (Martinez-Martin *et al*, 2017). Briefly, we measured by flow cytometry the accumulation of vesicular LC3 using bafilomycin A1 (BafA1) or chloroquine, two commonly used autophagy inhibitors, which block LC3 degradation differently. The total autophagy flux was revealed as the mean fluorescence intensity (MFI) after chloroquine treatment, the canonical autophagy flux was detected as the MFI after BafA1 treatment, and the noncanonical autophagy flux as the difference between total and canonical, normalized by the MFI of LC3 before inhibitor treatment. *Listeria* exposure triggered a three-fold increase in non-canonical autophagy in BacB cells, compared to non-instructed B cells (Fig EV4A). This increase in non-canonical autophagy that was not observed when using *Listeria* Δhly, which maintain levels similar to those observed in non-instructed B cells (Fig EV4A). No differences were detected in any condition regarding canonical autophagy. Therefore *Listeria*-mediated instruction promote both, the increase non-canonical autophagy and antigen cross-presentation in BacB cells.

To further analyze whether *Listeria*-induced autophagy plays a determinant role in B cell instruction, BacB mediated cross-presentation was tested using B cells isolated from WT or its isogenic Atg16l1 KO mice (Conway *et al*, 2013). Deletion of Atg16l1 prevents the formation of the Atg12–Atg5-Atg16 complex. This conserved complex is essential for lipidation of LC3 during canonical and non-canonical autophagy, and consequently for autophagosome formation. Therefore, Atg16l1 is essential for autophagy induction (Walczak & Martens, 2013).

The antigen presentation ability of *Listeria*-OVA BacB cells was tested using B cells isolated from WT or Atg16l1 KO mice. Naïve OTI CD8$^+$ T cell proliferation was reduced drastically when the APC were Atg16l1 KO BacB cells (Fig EV4B and C). Acording to these data, H-2K$^b$ expression was also reduced in Atg16l1 KO BacB cells (Fig EV4D). Cell viability of Atg16l1 KO BacB cells was not reduced during the time of the experimentation (Fig EV4E). Together, these results show that non-canonical autophagy, plays a major role in bacteria-mediated antigen cross-presentation by BacB cells.

### BacB cells orchestrate cytotoxic responses *in vivo*

To further investigate the physiological role of BacB cell mediated antigen cross presentation *in vivo*, including its impact on CD8$^+$ T cell differentiation and bacterial challenge resolution, adoptive transfer assays were performed using Rag1$^{-/-}$ host mice (lymphocyte-deficient mice with intact innate immunity). The Rag1$^{-/-}$ mice were adoptively transferred with naïve CD8$^+$ T cells from wild type C57BL/6J mice, expressing the natural TCR repertoire together with: no B cells (group 1), B cells from WT mice (group2), B cells from Atg16l1 KO mice (group 3) or B cells from B2m KO mice (defective in MHC-I; group 4) (Fig 5A). Groups 3 and 4 were defective in antigen presentation. Mice from all groups were infected with a low (non-lethal) dose of *L. monocytogenes* ($10^3$ bacteria per mouse) 1 day after cellular transfer. Four weeks after the first bacterial challenge, all mice were re-challenged with sublethal dose ($10^5$ bacteria per mouse) of *L. monocytogenes*. The differentiation of CD8$^+$ T cells in memory precursor effector cells (MPECs;

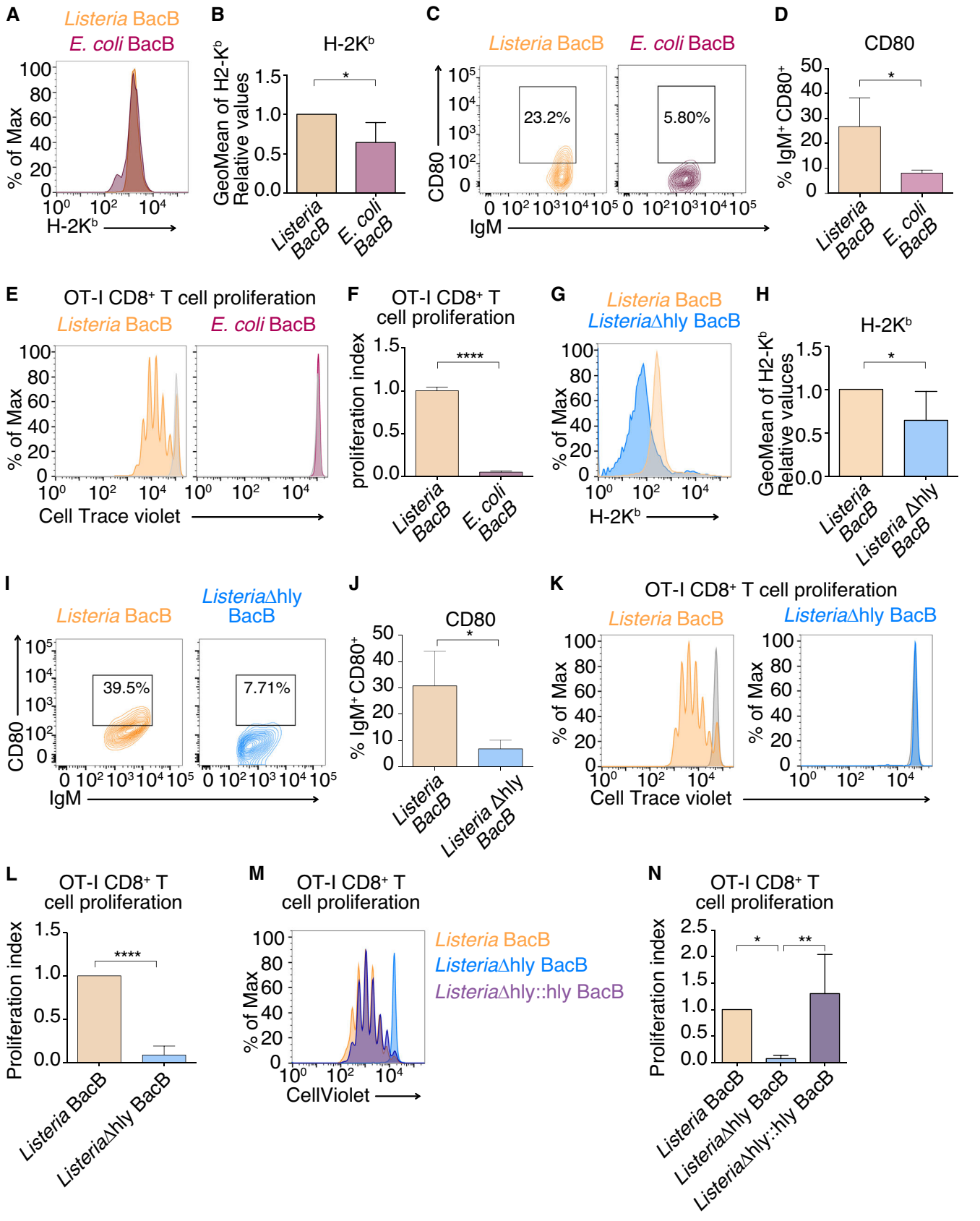


**Figure 4.**

**Figure 4. The capture of bacteria described to trigger autophagy are necessary for cross-presentation.**

A–D Surface expression of H-2K$^b$ (A, B) and CD80 (C, D) in *L. monocytogenes* (orange) or *E. coli* (purple) BacB cells analyzed by flow cytometry. (A and C) panels show representative experiments, (B and D) panels show the mean of at least three independent experiments.

E, F OTI CD8$^+$ T cells proliferation 3 days after activation with *Listeria*-OVA (E, left panel, orange) or *E. coli*-OVA (E, right panel, purple) BacB cells. Non-activated naïve CD8$^+$ T cells (gray) are shown as a negative proliferation control. (E) Panel show a representative experiment, (F) panel shows the proliferation index mean of at least three independent experiments.

G–J Surface expression of H-2K$^b$ (G, H) and CD80 (I, J) in *L. monocytogenes* (orange) or *L. monocytogenes* Δhly (blue) BacB cells analyzed by fow cytometry. (G and I) panels show a representative experiment, (H and J) panels show the mean of at least three independent experiments.

K Representative data showing OTI CD8$^+$ T cells proliferation 3 days after activation with *Listeria*-OVA (left panel, orange) or *Listeria* Δhly-OVA (right panel, blue) BacB cells. Non-activated naïve CD8$^+$ T cells (gray) are shown as a negative proliferation controls.

L Proliferation index mean of at least three experiments as in (K).

M Representative data showing OTI CD8$^+$ T cells proliferation 3 days after activation with *Listeria*-OVA (orange), *Listeria* Δhly-OVA (blue) or *Listeria* Δhly::hly-OVA BacB cells (Purple).

N Proliferation index mean of at least three experiments as in (H).

Data information: All B cells were isolated from WT mice. Column bars in the figure represent the mean. Error bars indicate the SD. Statistical significant differences, analyzed by *t*-test (two samples) or one way ANOVA (more than two samples), are represented by asterisk; *$P < 0.05$, **$P < 0.005$, ****$P < 0.00005$ non-significant differences are marked as (ns).
Source data are available online for this figure.

CD127$^{hi}$ KLRG1$^{lo}$), short-lived effector cells (SLECs; CD127$^{lo}$ KLRG1$^{hi}$) and early effector cells (EECs; CD127$^{lo}$ KLRG1$^{lo}$) was analyzed 2 days after bacterial re-challenge (Fig 5B–D). A significant increase in the EECs, a population with high plasticity described to increase after intracellular pathogen infections i.e. *Listeria* (Opata *et al*, 2015; Plumlee *et al*, 2015), was observed in the presence of WT B cells compared with the antigen presenting defective B cells.

These *in vivo* data confirm the active role of BacB dependent antigen cross-presentation in CD8$^+$ T cell differentiation after a *Listeria* challenge, and the role of autophagy in the BacB antigen cross-presentation process.

In view of these data, we investigated whether BacB mediated antigen cross-presentation plays a relevant role in controlling bacterial infections. Rag1$^{-/-}$ host mice were adoptively transferred with B cells from WT mice and Atg16l1 KO mice (antigen presentation-defective). The control mice were not transferred with any B cells. All the mice were simultaneously transferred with naïve CD8$^+$ T cells from wild type C57BL/6J mice, expressing the natural TCR repertoire. All groups were infected with a low (non-lethal) dose of *L. monocytogenes* ($10^3$ bacteria per mouse) 1 day after cellular transfer. Three weeks after first bacterial challenge, all the mice were re-challenged with a sublethal dose ($10^5$ bacteria per mouse) of *L. monocytogenes*. Two days after the bacterial re-challenge, the bacterial load in the liver was quantified by colony counting (Fig 5E).

In the absence of the B cells only half of the mice effectively responded to the challenge, maintaining a bacterial load lower than $10^5$ bacteria/g of liver, as a result of the action of their innate immunity and the CD8$^+$ T cells primed by innate immune cells i.e. DC. This result mimics which was observed in the presence of B cells with deficient antigen presentation abilities (B cells from Atg16l1 KO mice). Conversely, in the presence of WT B cells, all mice (100%) were able to control the bacterial challenge. These data show that B cell-dependent cross-priming of CD8$^+$ T cells improve the control of bacterial infections *in vivo*.

In addition, we tracked the survival of C57BL/6J mice during the time after they had been infected with a higher dose of *Listeria*. Note that in this experiment, we included an extra group which did not received any B, or CD8$^+$ T lymphocytes. In the conditions tested, it seems that the best survival line was observed when Rag1$^{-/-}$ mice had been transferred with WT B cells which were able to cross-present bacterial antigens, and naïve CD8$^+$ T cells (Fig 5F). However, when the B cells were unable to present antigens to CD8$^+$ T cells, the survival rate was very similar to that observed in the absence of B cells.

### BacB cells as a potential antitumor immunotherapy

We have therefore described a pathway for bacterial antigen acquisition by B cells and shown that BacB-mediated antigen cross-presentation plays an important role in activating *in vivo* CD8$^+$ T cells which are crucial for the improved control of intracellular bacterial infections. The "novel" abilities of BacB cells could have biomedical applications. For instance, the scientific community has striven to develop effective cellular immunotherapies based on T cell responses. Recent studies have shown that B and T cell infiltration correlate well with a with good prognosis in several cancers such as, melanoma, sarcoma or renal cell carcinoma (Nielsen *et al*, 2012; Garnelo *et al*, 2017; Edin *et al*, 2019; Cabrita *et al*, 2020; Helmink *et al*, 2020; Lu *et al*, 2020; Petitprez *et al*, 2020; Hu *et al*, 2021). Also, the ability of cross-present antigens by B cells provides a prospective tool for cancer immunotherapy (Shin *et al*, 2016; Possamaï *et al*, 2021). These observations led to further investigations into whether BacB cells could be used *in vivo* as potential novel antitumor therapy. As a proof-of-concept experiment, we tested BacB cell therapy in a model of aggressive murine melanoma.

We engineered a recombinant strain of *L. monocytogenes* to express murine tyrosinase-related protein-2 (TRP-2). TRP2 is a non-mutated melanocyte-derived differentiation antigen which is highly expressed in melanomas (Bloom *et al*, 1997). The rationale behind this investigation was that our previous data suggested that BacB cells might cross-present TRP2 antigen and trigger CD8$^+$ T cells responses against TRP2 expressing tumor cells.

B16 F10 melanoma cells were implanted subcutaneously in immune competent C57BL/6J mice. The mice were treated with the vehicle (PBS1x) or *Listeria*-TRP2 BacB cells for 3 consecutive days, 6 days after tumor implantation, when the tumors were formed and clearly visible (Fig 5G). BacB cells treatment greatly reduced the melanoma tumor size (Fig 5H and I). This highlights BacB cells as potential novel tool for cancer immunotherapy.

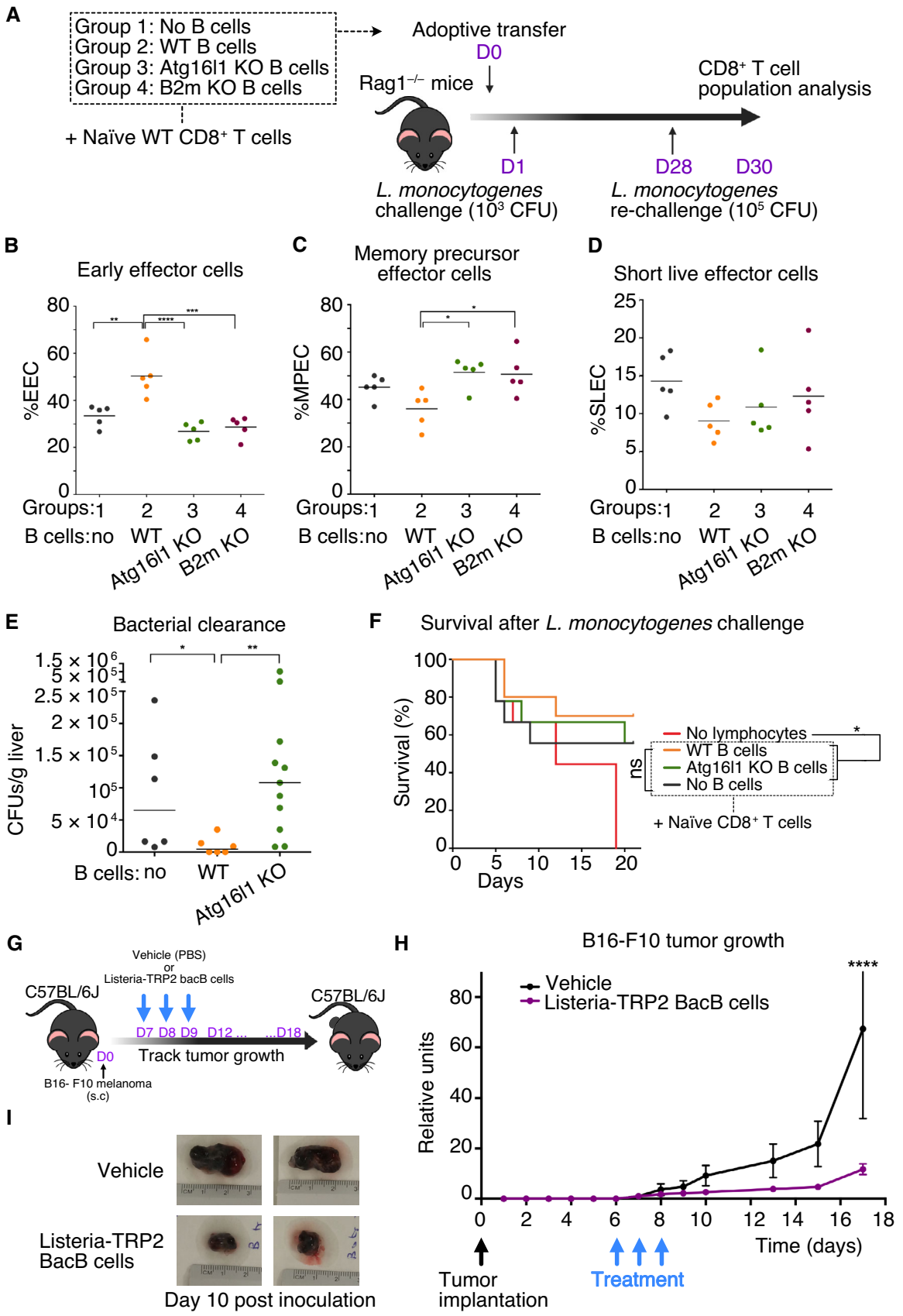


**Figure 5.**

**Figure 5. BacB cells orchestrate protective cytotoxic responses *in vivo*.**

A Experimental design to test the role of the antigen presenting ability of BacB cells to activate and differentiate naïve $CD8^+$ T cells in the context of bacterial challenge.

B–D Differentation of different $CD8^+$ T cell populations ((B) early effector cells, EECs ($CD127^{lo}$ $KLRG1^{lo}$); (C) memory precursor effector cells, MPECs ($CD127^{hi}$ $KLRG1^{lo}$); (D) short-lived effector cells, SLECs ($CD127^{lo}$ $KLRG1^{hi}$)), gated on $CD3^+CD8^+$ T cells in the presence of the indicated B cells, 2 days after a second bacterial rechallenge (as indicated in A).

E *L. monocytogenes* load in liver 2 days after a second bacterial challenge (30 days after the first challege) in the presence of the indicated B cells.

F Kaplan Meier survival curve of $Rag1^{-/-}$ mice after adoptive transfer and bacteria challenge.

G Experimental design to test whether BacB cell therapy could activate tumor-recognizing $CD8^+$ T cells that would fight against already implanted tumors in immunocopentent aimals.

H BacB cells reduce melanoma growth. B16 F10 melanoma cells ($4 \times 10^5$) were injected s.c. in the mid-right flank of C57BL/6J (WT) host mice (4 mice/group; treated with BacB or untreated). Once tumors were formed and visible (6 days after imlantation) mice were treated with *Listeria* TRP2 BacB cells or with vehicle (PBS) (three consecutive injections in 3 days). Tumor growth were monitored every 1–3 days. It is shown the mean and the SD of the tumor volume in each group at the indicated time points. Mice with tumors $\geq$ 300 $mm^3$ were sacrified.

I Representative tumors extracted 10 days post-implantation from animals treated with *Listeria*-TRP2 BacB cells or utreated (vehicle) controls.

Data information: Bars in the figure represent the mean. Error bars indicate the SD. Statistical significant differences, analyzed by ANOVA are represented by asterisk; $*P < 0.05$, $**P < 0.005$, $***P < 0.0005$, $****P < 0.00005$ non-significant differences are marked as (ns).
Source data are available online for this figure.

## Materials and Methods

### Mice

Wild-type (WT) C57BL/6J mice (RRID: IMSR_JAX:000664), C57BL/6-Tg (TcraTcrb)1100Mjb/J OT-I mice expressing TCR specific for OVA peptide 257–264 (SIINFEKL) in the context of H-$2K^b$ (RRID: IMSR_JAX:003831), C57BL/6J 129S7-Rag1tm1Mom/J ($Rag1^{-/-}$) mice, which lack B and T lymphocytes (RRID:IMSR_JAX:002216), were from Jackson Laboratory. C57BL/6-Tg(IghelMD4)4Ccg/J (JAX stock #002595; Mason *et al*, 1992) MD4 mice expressing BCR specific for HEL were kindly provided by Dr. Yolanda Carrasco (CNB-CSIC, Madrid), C57BL/6J 129S2-Tap1tm1Arp/J ($Tap1^{-/-}$) mice were kindly provided by Dr. Margarita del Val (CBM, Madrid). $Atg16l1^{f/f}$KO and $Atg16l1^{f/f}$ mice (Conway *et al*, 2013) were kindly provided by Dra. Nuria Martín Martinez (CBM). $Atg16l1^{f/f}$ mice were used as WT mice in all experiments including Atg16l1 KO mice.

For Atg16l1 gene deletion, $Atg16l1^{f/f}$KO mice and the corresponding controls $Atg16l1^{f/f}$ mice were treated with i.p. doses of 1 mg of Tamoxifen (Sigma) consecutively during 3 days. Seven days after the last dose, mice were treated with a unique booster dose of Tamoxifen. Six to seven days after the last dose, the animals were tested for effective gene deletion and used for experiments.

Male or female mice aged 8–12 weeks were used for experiments. Mice were maintained at the Centro Nacional de Biotecnología (CNB, Madrid) animal facilities and for some experiments in the SPF unit at the Centro Nacional de Investigaciones Cardiovasculares (CNIC, Madrid).

Experimental groups were assigned randomly and measurements made in a double-blind manner.

Experimental procedures were approved by the Committee for Research Ethics of CNB-CSIC and CNIC, and experiments were conducted in accordance with Spanish and EU guidelines. All procedures were approved by the Madrid local authority (project no PROEX 431/15).

### Bacterial strains

Bacterial strains used were *L. monocytogenes* 10403S (*Listeria*-WT) and *L. monocytogenes* 10403SΔhly (*Listeria*-Δhly) that were kindly provided by Prof. DA. Portnoy (University of California). In this work, we generated *Listeria*-OVA *Listeria* Δhly OVA and *Listeria* Δhly::hly OVA. The gene encoding for OVA was cloned in pPL2 insertion plasmid (Lauer *et al*, 2002) under the p60 promoter (generating pPL2OVA that was electroporated in *L. monocytogenes* 10403SΔhly or their isogenic *L. monocytogenes* 10403S). To recover LLO expression, OVA gene was cloned in pPL2 plasmid including the hly promoter and the gene part deleted in the 10403SΔhly strain (Riedel *et al*, 2007). LLO expression were checked by Western blotting (Fig EV3F). Bacteria were grown in brain-heart infusion (BHI) medium (overnight, 37°C). *E. coli* K12 MG1655 were kindly provided by Dr. LA. Fernández-Herrero (CNB-CSIC). This strain was transformed with the pGEN22-OVA plasmid to generate *E. coli* OVA. pGEN22 is a multicopy plasmid, containing a toxin-antitoxin system that prevent plasmid elimination, therefore suitable for *in vivo* experiments. OVA gene was cloned under the constitutive pOmpC promoter. To generate the *E. coli* OVA, TSS transformation was followed (Chung *et al*, 1989). Once transformed, bacteria were grown at 37°C in LB supplemented with 100 μg/ml ampicillin. All bacteria samples were washed in PBS before used for the experiments.

### Cells

Bone marrow dendritic cells (BM-DCs) were generated as described (Inaba *et al*, 1992). Briefly, cells from mouse bone marrow were incubated with recombinant murine granulocyte–macrophage colony-stimulating factor (rm-GM-CSF, 20 ng/ml) for 8–11 days, replacing the medium every 3 days. Maturation was induced the day before infection by adding to the medium 20 ng/ml lipopolysaccharide (LPS; overnight).

Primary conventional splenic B cells were obtained from single-cell suspensions of spleen through negative selection with the MojoSort™ Mouse Pan B Cell Isolation Kit (Biolegend). Cell suspensions were incubated with the biotin antibody cocktail plus anti- biotinCD11b (BD) followed by incubation with magnetic Streptavidin Nanobeads. The magnetic labeled fraction, retained by the use of a magnetic separator, was discarded and the untouched B cells were collected from the supernatant for experiments.

To isolate naïve $CD8^+$ T cells, splenic cell suspensions were incubated with the MojoSort™ mouse Naïve $CD8^+$ T cell Isolation Kit (Biolegend) as described for B cells.

All cells, including cell lines EL-4 lymphoma, HeLa and the B16 F10 melanoma were maintained at 37°C in RPMI 1640 medium (Fisher Scientific) supplemented with 10% fetal bovine serum (FBS), 0.1 U/ml penicillin, 0.1 mg/ml streptomycin (Lonza) and 0.05 mM 2-mercaptoethanol, in a humid atmosphere with 5% $CO_2$.

### Reagents

OVAp-I (OVA 257–264; SIINFEKL) was generated at Centro Nacional de Biotecnología (CNB-CSIC, Madrid). Other reagents were: Hen Egg Lysozyme (HEL) (Sigma-Aldrich), dynasore (Sigma-Aldrich), chloroquine (Sigma-Aldrich), mouse recombinant GM-CSF (Peprotech), LPS (Sigma-Aldrich), poly-L-lysine (Sigma-Aldrich), Gentamicin (Sigma-Aldrich).

### Gentamicin survival assay

To determine the number of bacteria entering the cells, we followed the method as described (Cruz-Adalia *et al*, 2014) with some modifications. BM-DCs were infected with the indicated bacteria at MOI of 20 for 1 h at 37°C. Then the medium was washed three times with PBS to remove free extracellular bacteria. Later on, B cells were added (1:1 B/DC ratio) and after 30 min of B cell-iDCs co-culture, 100 μg/ml of gentamicin was added, and samples were incubated for an additional 1 h at 37°C (in the case of *E. coli*, 200 μg/ml of gentamicin were used). Then, samples were washed three times with PBS to remove the antibiotic and B cells were re-isolated by either cell sorting or magnetic separation. Purified B cells were lysed with 0.05% Triton X-100 (Sigma-Aldrich) in distilled water. Dilutions were seeded in LB (*E. coli*) or BHI (*L. monocytogenes*) agar containing Petri dishes. Bacteria colonies were visualized and quantified one (*E. coli*) or 2 days (*L. monocytogenes*) later.

### Bacterial instruction

Spleen purified B cells were added to plates containing previously washed, bacteria-infected BM-DCs. Three hours after DC/B-cell contacts, gentamicin (100 μg/ml) was added to cultures and left O/N. Twenty-four hours after cell co-culture, B cells were purified by cell sorting ($CD11c^-$ $IgM^+$; Fig EV2A) or negative selection kit and magnetic separator as indicated before. Purified B cells were considered BacB cells and used in different assays. B cells from MD4 mice and HEL-decorated DC were used in experiments shown in Figs 1–3. As, transphagocytosis does not require BCR activation, experiments from Fig 3G to the end of the manuscript were performed using B cells from WT or the indicated animals, in absence HEL-mediated BCR activation. Note that during B cells instruction process more that 90% of the DC died (Fig EV2B).

### Immunofluorescence microscopy

B cells and infected BM-DCs were co-culture during the indicated times. Gentamicin was added to avoid extracellular bacterial growth. Samples were fixed with 4% paraformaldehyde in PBS after 30 min or 2 h of culture. B cells were prestained with CellTrace Violet.

BacB cells and naïve $CD8^+$ T cells were allowed to form conjugates (2 h), then fixed with 4% paraformaldehyde in PBS. $CD8^+$ T cells were prestained with CellTrace Violet.

Samples were permeabilized with 0.1% Triton X-100 in PBS before staining with indicated antibodies (Table 1). F-actin was detected using fluorescently tagged phalloidin. Samples were visualized by confocal microscopy (Leica TCS-SP5; ×63 lens, controlled by Leica LAS AF). Images were analyzed with FIJI (ImageJ) software (NIH).

### Quantification the actin accumulation at the IS

Cellular contacts between BacB cells and naïve $CD8^+$ T cells were visualized by confocal microscopy as described above. In order to quantify the amount of actin accumulated at the IS, confocal images were analyzed using the plugin *Synapse measures* in ImageJ. Synapse measures accurately quantify the ratio between the immunofluorescence intensity of $CD8^+$ T-cell actin at the IS with that remained in the rest of the $CD8^+$ T cell (and taking into account the actin present in the BacB cells and the background signal). A detailed description of the Synapse Measures program, including the algorithms used, is described in (Calabia-Linares *et al*, 2011). The tutorial and the link to freely download the plugin are in this url: https://github.com/anaacayuela/SynapseMeasures.

### $CD8^+$ T-cell proliferation assays

Cell sorter-purified (or magnetic negatively isolated) BacB cells were incubated with naive OT-I $CD8^+$ T cells, previously stained with CellTrace Violet to quantify their proliferation by flow cytometry. In every cell division, the proliferating cells diluted the staining, observed as a shift to the left in the histogram; only live cells (negatively stained for 7AAD or Live/Dead Fixable Viability Near-IR)

**Table 1. Antibodies used for immunofluorescence.**

| Reactivity | Conjugated | Dilution | Source |
|---|---|---|---|
| CD3ζ | - | 1:200 | Donated by Prof. B. Alarcon (CBM-SO, Madrid) |
| *L. monocytogenes* | - | 1:200 | AbD Serotec |
| *E. coli* | - | 1:200 | AbD Serotec |
| *L. monocytogenes* | APC | 1:100 | Novus Biologicals |
| Phalloidin | Alexa Fluor 488 | 1:100 | Thermo Fisher Scientific |
| Phalloidin | TRITC | 1:100 | Thermo Fisher Scientific |
| Phalloidin | Alexa Fluor 660 | 1:100 | Thermo Fisher Scientific |
| LC3b | - | 1:100 | Cell Signaling |
| Goat-anti-Rabbit | Alexa Fluor 488 | 1:200 | Thermo Fisher Scientific |
| Goat-anti-Rabbit | Alexa Fluor 546 | 1:200 | Thermo Fisher Scientific |
| Goat-anti-Rabbit | Alexa Fluor 647 | 1:200 | Thermo Fisher Scientific |

**Table 2. Antibodies used for western blotting.**

| Reactivity | Dilution | Source |
|---|---|---|
| LC3b | 1:1,000 | Cell Signaling |
| ERK | 1:200 | Santa Cruz |
| TRP2 | 1:200 | Santa Cruz |
| LLO | 1:3,000 | Diatheva |
| Rabbit-HRP | 1:20,000 | Sigma-Aldrich |

were analyzed (Fig EV2C). As positive controls, OT-I $CD8^+$ T cells were incubated with OVAp-I-loaded BM-DC or with antibodies activating CD3 (clone 17A2, eBioscience; 5 μg/ml, coated on plate) and CD28 (clone 37.51, BD Pharmingen, soluble 2 μg/ml).

### Cytotoxicity assay

Effector cytotoxic $CD8^+$ T cells were prepared from naïve $CD8^+$ T cells isolated from spleen of OT-I mice, and activated with *Listeria*-OVA BacB cells, or with OVAp-I-loaded splenocytes as positive control, during 7 days.

EL-4 cells were incubated alone or with 0.5 μM OVAp-I for 1 h. After washing with PBS, OVAp-I-loaded EL-4 cells were stained with 5 μM CellTrace Violet and unloaded EL-4 cells with 0.5 μM CellTrace Violet. After washing with complete medium (with FBS), the populations were mixed and incubated with CTL at various ratios (5:1, 2:1, 1:1, 0.5:1 EL-4:CTL; for 4 h). Next, they were analyzed by flow cytometry. Specific cytotoxicity was calculated as $1 - (\%\ \text{EL-4 CellViolet}^{high}/\%\ \text{EL-4 CellViolet}^{low}) \times 100$ (Lang *et al*, 2005). Relative cytotoxicity was calculated by subtracting the specific cytotoxicity of the negative control (EL-4 cells incubated without CTL).

### Western blotting

Proteins of bacteria or cell lysates were separated by standard procedures on SDS-PAGE gels (Mini-PROTEAN TGX, Biorad) and transferred onto Trans-Blot Turbo PVDF membrane (Biorad). Membranes were blocked for 1 h in 5% BSA and then probed with the correspond antibodies (see Table 2).

### Autophagy flux

After bacteria-instruction protocol, BacB cells were left untreated or incubated with chloroquine or bafilomycin for 2 h. After this time, cells were processed using Guava autophagy LC3 antibody-based detection kit following manufacture instructions. Afterwards, vesicular LC3 levels were detected by flow cytometry and LC3 mean

**Table 3. Antibodies and probes used for flow cytometry.**

| Reactivity | Clone | Conjugated | Dilution | Source |
|---|---|---|---|---|
| CD19 | 6D5 | Allophycocyanin | 1:200 | Southern biotech |
| CD19 | 6D5 | Phycoerythrin | 1:200 | Southern biotech |
| IgM | Polyclonal | Fluorescein isothiocyanate | 1:100 | Southern biotech |
| CD8a | 53-6.7 | Fluorescein isothiocyanate | 1:100 | Tonbo Biosciences |
| CD8a | 53-6.7 | Phycoerythrin | 1:100 | BD Biosciences |
| CD25 | PC61.5 | Allophycocyanin | 1:200 | Tonbo Biosciences |
| CD3 | 145-2C11 | PECy7 | 1:100 | Biolegend |
| CD5 | | PercpCy5.5 | 1:100 | eBiosciences |
| CD127 | A7R34 | Brillant Violet | 1:200 | Biolegend |
| KLRG1 | 2F1 | Allophycocyanin | 1:100 | BD Pharmigen |
| CD11c | N418 | Phycoerythrin | 1:200 | Tonbo Biosciences |
| Iale | 2G9 | Fluorescein isothiocyanate | 1:200 | BD Biosciences |
| Gr-1 | RB6-8C5 | Allophycocyanin | 1:100 | Tonbo Biosciences |
| CD86 | | Phycoerythrin | 1:100 | |
| CD80 | GL-1 | Phycoerythrin | 1:100 | Biolegend |
| H-$2K^b$ | AF6-88.5 | Phycoerythrin | 1:100 | BD Biosciences |
| SIINFEKL/H-$2K^b$ | eBio25-D1.16 | Allophycocyanin | 1:50 | eBioscience |
| IFNγ | XMG1.2 | Allophycocyanin | 1:100 | BD Pharmigen |
| LIVE/DEAD® Fixable Near-IR Dead Cell Stain Kit | | 750/775 | 1:1,000 | ThermoFisher |
| CYTO-ID® Autophagy detection kit | | 488 | 1:1,000 | Enzo |
| 7-AAD Viability Staining Solution | | 546/647 | 1:1,000 | eBiosciences |
| CellTrace™ Violet | | 415/516 | 1:1,000 | ThermoFisher |
| Cell Proliferation Kit | | | | |
| CD16/CD32 | 2.4 G2 | | 1:200 | BD Bioscience |

fluorescence levels were used to calculate total autophagy, non-canonical autophagy and canonical autophagy relative levels as described in (Martinez-Martin *et al*, 2017).

#### Anti-tumor assay

B16 F10 melanoma cells ($4 \times 10^5$) were injected subcutaneously (s.c) into the mid-right flank of C57BL/6J recipient mice and adoptively transferred with BacB cells as therapeutic treatment when tumors were already implanted and clearly visible (at days 6, 7 and 8). Mice were divided into two groups, control treated i.v. with PBS (group 1) and adoptively transferred i.v with $10^6$ *Listeria*-TRP2 BacB cells (group 2). Tumor growth were tracked every 2 days with a dial caliper. Experimental groups were assigned randomly and measurements made in a double-blind manner.

#### Analysis of $CD8^+$ T cell populations during *Listeria* infection

Rag-$1^{-/-}$ recipient mice were divided into four experimental groups; mice were injected i.v. with PBS (Group 1), $5 \times 10^5$ naïve $CD8^+$ T cells from WT mice (Group 2), $5 \times 10^5$ naïve $CD8^+$ T cells from WT mice plus $10^6$ B cells from Atg16l1$^{f/f}$ (WT) mice (Group 3), $5 \times 10^5$ naïve $CD8^+$ T cells from WT mice plus $10^6$ B cells from Atg16l1$^{f/f}$ KO mice (Group 4). One day after cell transfer, *L. monocytogenes* was injected i.v. ($10^3$ bacteria per mouse). The mice received a second challenge 30 days later of $2 \times 10^5$ *L. monocytogenes*; after 2 days, bacteria load in the liver were analyzed by bacteria platting and CFUs count. Moreover, splenocytes were stained with antibodies to CD8, CD3, CD127 and KLRG1 conjugated with several fluorochromes (see Table 3).

#### Determination of live bacteria in the liver

As described above, 2 days after re-challenge, harvested livers were individually weighed, placed in PBS and homogenized with ultra turrax homogenizer. The suspensions were serially diluted and plated on BHI agar plates and colonies counted after overnight incubation at 37°C. Bacterial load was expressed as CFU per gram of liver.

#### Statistical analysis

All statistical analyzes were performed using GraphPad Prism software. When analyzing more than two groups, we used one-way analysis of variance (ANOVA), and multiple mean comparisons were corrected with Tukey post-test. Student's *t*-test was used when individual comparisons of the mean between two groups were performed. Differences were considered significant at *P*-value = 0.05. Data are shown in column bars representing the mean ± SD of at least three independent experiments unless otherwise indicated.

## Data availability

No data have been deposited in public repositories.

**Expanded View** for this article is available online.

### Acknowledgements

We are grateful to advanced light microscopy and cytometry facilities of CNB for technical supporting. The research is supported by grants: SAF2017-84091-R, and PID2020-116393RB-I00/AEI/10.13039/501100011033, financed by MCIN, BFERO2020.04, financed by FERO foundation and PI20/0036 from ISCIII. RGF is supported by BES-2016-076526 from the Spanish Ministry of Economy Industry and Competitiveness, JOP is supported by fellowship LCF/BQ/SO16/52270012 from *La Caixa*, BHF is supported by FPU18/00895 and AMP by FPU18/03199 from Ministry of Science, Innovation and Universities. LdC has been supported by Juan de la Cierva grant IJC2018-035386-I and a contract associated to SEV-2017-0712. EVC, AMP, AMAM, and NMM belong to the Spanish National Research Council (CSIC)'s Cancer Hub. Synopsis image made with biorender.com by Eduardo Román Camacho and Esteban Veiga. We thanks Prof. Dan Portnoy who kindly provided bacterial strains.

### Author contributions

**Raquel García-Ferreras:** Data curation; formal analysis; supervision; validation; investigation; visualization; methodology; writing – original draft. **Jesús Osuna-Pérez:** Investigation; methodology. **Guillermo Ramírez-Santiago:** Supervision; validation; investigation; methodology. **Almudena Méndez-Pérez:** Supervision; investigation; methodology. **Andrés M Acosta-Moreno:** Methodology. **Lara Del Campo:** Methodology. **María J Gómez-Sánchez:** Methodology. **Marta Iborra:** Methodology. **Beatriz Herrero-Fernández:** Methodology. **José M González-Granado:** Methodology. **Francisco Sánchez-Madrid:** Investigation. **Yolanda R Carrasco:** Supervision; validation; writing – review and editing. **Patricia Boya:** Supervision; writing – review and editing. **Nuria Martínez-Martín:** Validation; investigation; methodology; writing – review and editing. **Esteban Veiga:** Conceptualization; resources; data curation; formal analysis; supervision; funding acquisition; validation; investigation; visualization; methodology; writing – original draft; project administration; writing – review and editing.

### Disclosure and competing interests statement

The authors declare that they have no conflict of interest.

## References

Akkaya M, Kwak K, Pierce SK (2020) B cell memory: building two walls of protection against pathogens. *Nat Rev Immunol* 20: 229 – 238

Allen CDC, Okada T, Tang HL, Cyster JG (2007) Imaging of germinal center selection events during affinity maturation. *Science* 315: 528 – 531

Alloatti A, Kotsias F, Pauwels A-M, Carpier J-M, Jouve M, Timmerman E, Pace L, Vargas P, Maurin M, Gehrmann U *et al* (2015) Toll-like receptor 4 engagement on dendritic cells restrains phago-lysosome fusion and promotes cross-presentation of antigens. *Immunity* 43: 1087 – 1100

Anand PK, Tait SWG, Lamkanfi M, Amer AO, Nunez G, Pagès G, Pouysségur J, McGargill MA, Green DR, Kanneganti T-D (2011) TLR2 and RIP2 pathways mediate autophagy of *Listeria monocytogenes* via extracellular signal-regulated kinase (ERK) activation. *J Biol Chem* 286: 42981 – 42991

Barbet G, Nair-Gupta P, Schotsaert M, Yeung ST, Moretti J, Seyffer F, Metreveli G, Gardner T, Choi A, Tortorella D *et al* (2021) TAP dysfunction in dendritic cells enables noncanonical cross-presentation for T cell priming. *Nat Immunol* 22: 497 – 509

Blander JM (2018) Regulation of the cell biology of antigen cross-presentation. *Annu Rev Immunol* 36: 717 – 753

Bloom MB, Perry-Lalley D, Robbins PF, Li Y, El-Gamil M, Rosenberg SA, Yang JC (1997) Identification of tyrosinase-related protein 2 as a tumor rejection antigen for the B16 melanoma. *J Exp Med* 185: 453 – 459

Cabrita R, Lauss M, Sanna A, Donia M, Skaarup Larsen M, Mitra S, Johansson I, Phung B, Harbst K, Vallon-Christersson J *et al* (2020) Tertiary lymphoid structures improve immunotherapy and survival in melanoma. *Nature* 577: 561 – 565

Calabia-Linares C, Robles-Valero J, de la Fuente H, Perez-Martinez M, Martín-Cofreces N, Alfonso-Pérez M, Gutierrez-Vázquez C, Mittelbrunn M, Ibiza S, Urbano-Olmos FR *et al* (2011) Endosomal clathrin drives actin accumulation at the immunological synapse. *J Cell Sci* 124: 820 – 830

Campisi L, Soudja SM, Cazareth J, Bassand D, Lazzari A, Brau F, Narni-Mancinelli E, Glaichenhaus N, Geissmann F, Lauvau G (2011) Splenic CD8α$^+$ dendritic cells undergo rapid programming by cytosolic bacteria and inflammation to induce protective CD8$^+$ T-cell memory. *Eur J Immunol* 41: 1594 – 1605

Canton J, Blees H, Henry CM, Buck MD, Schulz O, Rogers NC, Childs E, Zelenay S, Rhys H, Domart M-C *et al* (2021) The receptor DNGR-1 signals for phagosomal rupture to promote cross-presentation of dead-cell-associated antigens. *Nat Immunol* 22: 140 – 153

Carrasco YR, Batista FD (2007) B cells acquire particulate antigen in a macrophage-rich area at the boundary between the follicle and the subcapsular sinus of the lymph node. *Immunity* 27: 160 – 171

Cerovic V, Houston SA, Westlund J, Utriainen L, Davison ES, Scott CL, Bain CC, Joeris T, Agace WW, Kroczek RA *et al* (2015) Lymph-borne CD8α$^+$ dendritic cells are uniquely able to cross-prime CD8$^+$ T cells with antigen acquired from intestinal epithelial cells. *Mucosal Immunol* 8: 38 – 48

Chávez-Arroyo A, Portnoy DA (2020) Why is *Listeria monocytogenes* such a potent inducer of CD8$^+$ T-cells? *Cell Microbiol* 22: e13175

Chung CT, Niemela SL, Miller RH (1989) One-step preparation of competent *Escherichia coli*: transformation and storage of bacterial cells in the same solution. *Proc Natl Acad Sci USA* 86: 2172 – 2175

Colluru VT, McNeel DG (2016) B lymphocytes as direct antigen-presenting cells for anti-tumor DNA vaccines. *Oncotarget* 7: 67901 – 67918

Conway KL, Kuballa P, Song J-H, Patel KK, Castoreno AB, Yilmaz OH, Jijon HB, Zhang M, Aldrich LN, Villablanca EJ *et al* (2013) Atg16l1 is required for autophagy in intestinal epithelial cells and protection of mice from Salmonella infection. *Gastroenterology* 145: 1347 – 1357

Crotty S (2019) T follicular helper cell biology: a decade of discovery and diseases. *Immunity* 50: 1132 – 1148

Cruz-Adalia A, Ramirez-Santiago G, Calabia-Linares C, Torres-Torresano M, Feo L, Galán-Díez M, Fernández-Ruiz E, Pereiro E, Guttmann P, Chiappi M *et al* (2014) T cells kill bacteria captured by transinfection from dendritic cells and confer protection in mice. *Cell Host Microbe* 15: 611 – 622

Cruz-Adalia A, Ramirez-Santiago G, Osuna-Pérez J, Torres-Torresano M, Zorita V, Martínez-Riaño A, Boccasavia V, Borroto A, Martínez Del Hoyo G, González-Granado JM *et al* (2017) Conventional CD4$^+$ T cells present bacterial antigens to induce cytotoxic and memory CD8$^+$ T cell responses. *Nat Commun* 8: 1591

de Wit J, Souwer Y, Jorritsma T, Klaasse Bos H, ten Brinke A, Neefjes J, van Ham SM (2010) Antigen-specific B cells reactivate an effective cytotoxic T cell response against phagocytosed salmonella through cross-presentation. *PLoS One* 5: e13016

Dustin ML, Depoil D (2011) New insights into the T cell synapse from single molecule techniques. *Nat Rev Immunol* 11: 672 – 684

Edin S, Kaprio T, Hagström J, Larsson P, Mustonen H, Böckelman C, Strigård K, Gunnarsson U, Haglund C, Palmqvist R (2019) The prognostic importance of CD20$^+$ B lymphocytes in colorectal cancer and the relation to other immune cell subsets. *Sci Rep* 9: 19997

English L, Chemali M, Duron J, Rondeau C, Laplante A, Gingras D, Alexander D, Leib D, Norbury C, Lippé R *et al* (2009) Autophagy enhances the presentation of endogenous viral antigens on MHC class I molecules during HSV-1 infection. *Nat Immunol* 10: 480 – 487

Fleire SJ, Goldman JP, Carrasco YR, Weber M, Bray D, Batista FD (2006) B cell ligand discrimination through a spreading and contraction response. *Science* 312: 738 – 741

Gao J, Ma X, Gu W, Fu M, An J, Xing Y, Gao T, Li W, Liu Y (2012) Novel functions of murine B1 cells: active phagocytic and microbicidal abilities. *Eur J Immunol* 42: 982 – 992

Garnelo M, Tan A, Her Z, Yeong J, Lim CJ, Chen J, Lim KH, Weber A, Chow P, Chung A *et al* (2017) Interaction between tumour-infiltrating B cells and T cells controls the progression of hepatocellular carcinoma. *Gut* 66: 342 – 351

Garside P, Ingulli E, Merica RR, Johnson JG, Noelle RJ, Jenkins MK (1998) Visualization of specific B and T lymphocyte interactions in the lymph node. *Science* 281: 96 – 99

Gaspar M, May JS, Sukla S, Frederico B, Gill MB, Smith CM, Belz GT, Stevenson PG (2011) Murid herpesvirus-4 exploits dendritic cells to infect B cells. *PLoS Pathog* 7: e1002346

Germic N, Frangez Z, Yousefi S, Simon H-U (2019) Regulation of the innate immune system by autophagy: monocytes, macrophages, dendritic cells and antigen presentation. *Cell Death Differ* 26: 715 – 727

Gonzalez SF, Lukacs-Kornek V, Kuligowski MP, Pitcher LA, Degn SE, Kim Y-A, Cloninger MJ, Martinez-Pomares L, Gordon S, Turley SJ *et al* (2010) Capture of influenza by medullary dendritic cells via SIGN-R1 is essential for humoral immunity in draining lymph nodes. *Nat Immunol* 11: 427 – 434

Gordon S (2016) Phagocytosis: an immunobiologic process. *Immunity* 44: 463 – 475

Gutierrez MG, Master SS, Singh SB, Taylor GA, Colombo MI, Deretic V (2004) Autophagy is a defense mechanism inhibiting BCG and *Mycobacterium tuberculosis* survival in infected macrophages. *Cell* 119: 753 – 766

Heit A, Huster KM, Schmitz F, Schiemann M, Busch DH, Wagner H (2004) CpG-DNA aided cross-priming by cross-presenting B cells. *J Immunol* 172: 1501 – 1507

Helmink BA, Reddy SM, Gao J, Zhang S, Basar R, Thakur R, Yizhak K, Sade-Feldman M, Blando J, Han G *et al* (2020) B cells and tertiary lymphoid structures promote immunotherapy response. *Nature* 577: 549 – 555

Holl V, Xu K, Peressin M, Lederle A, Biedma ME, Delaporte M, Decoville T, Schmidt S, Laumond G, Aubertin A-M *et al* (2010) Stimulation of HIV-1 replication in immature dendritic cells in contact with primary CD4 T or B lymphocytes. *J Virol* 84: 4172 – 4182

Hon H, Oran A, Brocker T, Jacob J (2005) B lymphocytes participate in cross-presentation of antigen following gene gun vaccination. *J Immunol* 174: 5233 – 5242

Hu Q, Hong Y, Qi P, Lu G, Mai X, Xu S, He X, Guo Y, Gao L, Jing Z *et al* (2021) Atlas of breast cancer infiltrated B-lymphocytes revealed by paired single-cell RNA-sequencing and antigen receptor profiling. *Nat Commun* 12: 2186

Huppa JB, Davis MM (2003) T-cell-antigen recognition and the immunological synapse. *Nat Rev Immunol* 3: 973 – 983

Inaba K, Inaba M, Romani N, Aya H, Deguchi M, Ikehara S, Muramatsu S, Steinman RM (1992) Generation of large numbers of dendritic cells from mouse bone marrow cultures supplemented with granulocyte/macrophage colony-stimulating factor. *J Exp Med* 176: 1693 – 1702

Khanna KM, McNamara JT, Lefrançois L (2007) *In situ* imaging of the endogenous CD8 T cell response to infection. *Science* 318: 116 – 120

Krocova Z, Plzakova L, Pavkova I, Kubelkova K, Macela A, Ozanic M, Marecic V, Mihelcic M, Santic M (2020) The role of B cells in an early immune response to *Mycobacterium bovis*. *Microb Pathog* 140: 103937

 

Lang D, Lu MM, Huang L, Engleka KA, Zhang M, Chu EY, Lipner S, Skoultchi A, Millar SE, Epstein JA (2005) Pax3 functions at a nodal point in melanocyte stem cell differentiation. *Nature* 433: 884 – 887

Lauer P, Chow MYN, Loessner MJ, Portnoy DA, Calendar R (2002) Construction, characterization, and use of two *Listeria monocytogenes* site-specific phage integration vectors. *J Bacteriol* 184: 4177 – 4186

Levine LS, Hiam-Galvez KJ, Marquez DM, Tenvooren I, Madden MZ, Contreras DC, Dahunsi DO, Irish JM, Oluwole OO, Rathmell JC *et al* (2021) Single-cell analysis by mass cytometry reveals metabolic states of early-activated $CD8^+$ T cells during the primary immune response. *Immunity* 54: 829 – 844

Li J, Barreda DR, Zhang Y-A, Boshra H, Gelman AE, Lapatra S, Tort L, Sunyer JO (2006) B lymphocytes from early vertebrates have potent phagocytic and microbicidal abilities. *Nat Immunol* 7: 1116 – 1124

Liu W, Wang H, Xu C (2016) Antigen receptor nanoclusters: small units with big functions. *Trends Immunol* 37: 680 – 689

Lu Y, Zhao Q, Liao J-Y, Song E, Xia Q, Pan J, Li Y, Li J, Zhou B, Ye Y *et al* (2020) Complement signals determine opposite effects of B cells in chemotherapy-induced immunity. *Cell* 180: 1081 – 1097

Mariño E, Tan B, Binge L, Mackay CR, Grey ST (2012) B-cell cross-presentation of autologous antigen precipitates diabetes. *Diabetes* 61: 2893 – 2905

Martinez-Martin N, Maldonado P, Gasparrini F, Frederico B, Aggarwal S, Gaya M, Tsui C, Burbage M, Keppler SJ, Montaner B *et al* (2017) A switch from canonical to noncanonical autophagy shapes B cell responses. *Science* 355: 641 – 647

Martínez-Riaño A, Bovolenta ER, Mendoza P, Oeste CL, Martín-Bermejo MJ, Bovolenta P, Turner M, Martínez-Martín N, Alarcón B (2018) Antigen phagocytosis by B cells is required for a potent humoral response. *EMBO Rep* 19: e46016

Mason DY, Jones M, Goodnow CC (1992) Development and follicular localization of tolerant B lymphocytes in lysozyme/anti-lysozyme IgM/IgD transgenic mice. *Int Immunol* 4: 163 – 175

Mattila PK, Feest C, Depoil D, Treanor B, Montaner B, Otipoby KL, Carter R, Justement LB, Bruckbauer A, Batista FD (2013) The actin and tetraspanin networks organize receptor nanoclusters to regulate B cell receptor-mediated signaling. *Immunity* 38: 461 – 474

Menon A, Shroyer M, Wampler J, Chawan C, Bhunia A (2003) *In vitro* study of *Listeria monocytogenes* infection to murine primary and human transformed B cells. *Comp Immunol Microbiol Infect Dis* 26: 157 – 174

Meyer-Morse N, Robbins JR, Rae CS, Mochegova SN, Swanson MS, Zhao Z, Virgin HW, Portnoy D (2010) Listeriolysin O is necessary and sufficient to induce autophagy during *Listeria monocytogenes* infection. *PLoS One* 5: e8610

Mintern JD, Macri C, Chin WJ, Panozza SE, Segura E, Patterson NL, Zeller P, Bourges D, Bedoui S, McMillan PJ *et al* (2015) Differential use of autophagy by primary dendritic cells specialized in cross-presentation. *Autophagy* 11: 906 – 917

Mitchell G, Cheng MI, Chen C, Nguyen BN, Whiteley AT, Kianian S, Cox JS, Green DR, McDonald KL, Portnoy DA (2018) *Listeria monocytogenes* triggers noncanonical autophagy upon phagocytosis, but avoids subsequent growth-restricting xenophagy. *Proc Natl Acad Sci USA* 115: E210 – E217

Münz C (2016) Autophagy beyond intracellular MHC class II antigen presentation. *Trends Immunol* 37: 755 – 763

Natkanski E, Lee W-Y, Mistry B, Casal A, Molloy JE, Tolar P (2013) B cells use mechanical energy to discriminate antigen affinities. *Science* 340: 1587 – 1590

Nielsen JS, Sahota RA, Milne K, Kost SE, Nesslinger NJ, Watson PH, Nelson BH (2012) $CD20^+$ tumor-infiltrating lymphocytes have an atypical $CD27^-$ memory phenotype and together with $CD8^+$ T cells promote favorable prognosis in ovarian cancer. *Clin Cancer Res* 18: 3281 – 3292

Nutt SL, Hodgkin PD, Tarlinton DM, Corcoran LM (2015) The generation of antibody-secreting plasma cells. *Nat Rev Immunol* 15: 160 – 171

Ochando JC, Homma C, Yang Y, Hidalgo A, Garin A, Tacke F, Angeli V, Li Y, Boros P, Ding Y *et al* (2006) Alloantigen-presenting plasmacytoid dendritic cells mediate tolerance to vascularized grafts. *Nat Immunol* 7: 652 – 662

Opata MM, Carpio VH, Ibitokou SA, Dillon BE, Obiero JM, Stephens R (2015) Early effector cells survive the contraction phase in malaria infection and generate both central and effector memory T cells. *J Immunol* 194: 5346 – 5354

Paludan C, Schmid D, Landthaler M, Vockerodt M, Kube D, Tuschl T, Münz C (2005) Endogenous MHC class II processing of a viral nuclear antigen after autophagy. *Science* 307: 593 – 596

Parekh VV, Pabbisetty SK, Wu L, Sebzda E, Martinez J, Zhang J, Van Kaer L (2017) Autophagy-related protein Vps34 controls the homeostasis and function of antigen cross-presenting $CD8\alpha^+$ dendritic cells. *Proc Natl Acad Sci USA* 114: E6371 – E6380

Petitprez F, de Reyniès A, Keung EZ, Chen TW-W, Sun C-M, Calderaro J, Jeng Y-M, Hsiao L-P, Lacroix L, Bougoüin A *et al* (2020) B cells are associated with survival and immunotherapy response in sarcoma. *Nature* 577: 556 – 560

Pilli M, Arko-Mensah J, Ponpuak M, Roberts E, Master S, Mandell MA, Dupont N, Ornatowski W, Jiang S, Bradfute SB *et al* (2012) TBK-1 promotes autophagy-mediated antimicrobial defense by controlling autophagosome maturation. *Immunity* 37: 223 – 234

Plumlee CR, Obar JJ, Colpitts SL, Jellison ER, Haining WN, Lefrancois L, Khanna KM (2015) Early effector CD8 T cells display plasticity in populating the short-lived effector and memory-precursor pools following bacterial or viral infection. *Sci Rep* 5: 12264

Possamaï D, Pagé G, Panès R, Gagnon É, Lapointe R (2021) CD40L-stimulated B lymphocytes are polarized toward APC functions after exposure to IL-4 and IL-21. *J Immunol* 207: 77 – 89

Prokopec KE, Georgoudaki A-M, Sohn S, Wermeling F, Grönlund H, Lindh E, Carroll MC, Karlsson MCI (2016) Cutting edge: marginal zone macrophages regulate antigen transport by B cells to the follicle in the spleen via CD21. *J Immunol* 197: 2063 – 2068

Qi H, Egen JG, Huang AYC, Germain RN (2006) Extrafollicular activation of lymph node B cells by antigen-bearing dendritic cells. *Science* 312: 1672 – 1676

Ren H, Zhang T, Wang Y, Yao Q, Wang Z, Zhang L, Wang L (2021) Tumor-derived autophagosomes (DRibbles) activate human B cells to induce efficient antigen-specific human memory T-cell responses. *Front Immunol* 12: 675822

Riedel CU, Monk IR, Casey PG, Morrissey D, O'Sullivan GC, Tangney M, Hill C, Gahan CGM (2007) Improved luciferase tagging system for *Listeria monocytogenes* allows real-time monitoring *in vivo* and *in vitro*. *Appl Environ Microbiol* 73: 3091 – 3094

Robson NC, Donachie AM, Mowat AM (2008) Simultaneous presentation and cross-presentation of immune-stimulating complex-associated cognate antigen by antigen-specific B cells. *Eur J Immunol* 38: 1238 – 1246

Roozendaal R, Mempel TR, Pitcher LA, Gonzalez SF, Verschoor A, Mebius RE, von Andrian UH, Carroll MC (2009) Conduits mediate transport of low-molecular-weight antigen to lymph node follicles. *Immunity* 30: 264 – 276

Rosales-Reyes R, Pérez-López A, Sánchez-Gómez C, Hernández-Mote RR, Castro-Eguiluz D, Ortiz-Navarrete V, Alpuche-Aranda CM (2012)

Salmonella infects B cells by macropinocytosis and formation of spacious phagosomes but does not induce pyroptosis in favor of its survival. *Microb Pathog* 52: 367 – 374

Sánchez-Paulete AR, Teijeira A, Cueto FJ, Garasa S, Pérez-Gracia JL, Sánchez-Arráez A, Sancho D, Melero I (2017) Antigen cross-presentation and T-cell cross-priming in cancer immunology and immunotherapy. *Ann Oncol* 28: xii44 – xii55

Schmid D, Pypaert M, Münz C (2007) Antigen-loading compartments for major histocompatibility complex class II molecules continuously receive input from autophagosomes. *Immunity* 26: 79 – 92

Schriek P, Ching AC, Moily NS, Moffat J, Beattie L, Steiner TM, Hosking LM, Thurman JM, Holers VM, Ishido S *et al* (2022) Marginal zone B cells acquire dendritic cell functions by trogocytosis. *Science* 375: eabf7470

Shin C-A, Cho H-W, Shin A-R, Sohn H-J, Cho H-I, Kim T-G (2016) Co-expression of CD40L with CD70 or OX40L increases B-cell viability and antitumor efficacy. *Oncotarget* 7: 46173 – 46186

Souwer Y, Griekspoor A, de Wit J, Martinoli C, Zagato E, Janssen H, Jorritsma T, Bar-Ephraïm YE, Rescigno M, Neefjes J *et al* (2012) Selective infection of antigen-specific B lymphocytes by Salmonella mediates bacterial survival and systemic spreading of infection. *PLoS One* 7: e50667

Suzuki K, Grigorova I, Phan TG, Kelly LM, Cyster JG (2009) Visualizing B cell capture of cognate antigen from follicular dendritic cells. *J Exp Med* 206: 1485 – 1493

Tao S, Drexler I (2020) Targeting autophagy in innate immune cells: angel or demon during infection and vaccination? *Front Immunol* 11: 460

Tau GZ, Cowan SN, Weisburg J, Braunstein NS, Rothman PB (2001) Regulation of IFN-gamma signaling is essential for the cytotoxic activity of $CD8^+$ T cells. *J Immunol* 167: 5574 – 5582

Vidard L, Kovacsovics-Bankowski M, Kraeft SK, Chen LB, Benacerraf B, Rock KL (1996) Analysis of MHC class II presentation of particulate antigens of B lymphocytes. *J Immunol* 156: 2809 – 2818

Waite JC, Leiner I, Lauer P, Rae CS, Barbet G, Zheng H, Portnoy DA, Pamer EG, Dustin ML (2011) Dynamic imaging of the effector immune response to listeria infection *in vivo*. *PLoS Pathog* 7: e1001326

Walczak M, Martens S (2013) Dissecting the role of the Atg12-Atg5-Atg16 complex during autophagosome formation. *Autophagy* 9: 424 – 425

Wang Y-T, Zaitsev K, Lu Q, Li S, Schaiff WT, Kim K-W, Droit L, Wilen CB, Desai C, Balce DR *et al* (2020) Select autophagy genes maintain quiescence of tissue-resident macrophages and increase susceptibility to *Listeria monocytogenes*. *Nat Microbiol* 5: 272 – 281

Wculek SK, Cueto FJ, Mujal AM, Melero I, Krummel MF, Sancho D (2020) Dendritic cells in cancer immunology and immunotherapy. *Nat Rev Immunol* 20: 7 – 24

Wu T, Guan J, Handel A, Tscharke DC, Sidney J, Sette A, Wakim LM, Sng XYX, Thomas PG, Croft NP *et al* (2019) Quantification of epitope abundance reveals the effect of direct and cross-presentation on influenza CTL responses. *Nat Commun* 10: 2846

Yang J, Reth M (2010) The dissociation activation model of B cell antigen receptor triggering. *FEBS Lett* 584: 4872 – 4877

You Y, Myers RC, Freeberg L, Foote J, Kearney JF, Justement LB, Carter RH (2011) Marginal zone B cells regulate antigen capture by marginal zone macrophages. *J Immunol* 186: 2172 – 2181

Yuseff M-I, Reversat A, Lankar D, Diaz J, Fanget I, Pierobon P, Randrian V, Larochette N, Vascotto F, Desdouets C *et al* (2011) Polarized secretion of lysosomes at the B cell synapse couples antigen extraction to processing and presentation. *Immunity* 35: 361 – 374